Mammalian Target of Rapamycin (mTOR) Tagging Promotes Dendritic Branch Variability through the Capture of Ca²⁺/Calmodulin-dependent Protein Kinase II lpha (CaMKIIlpha) mRNAs by the RNA-binding Protein HuD*

Received for publication, July 28, 2014, and in revised form, May 1, 2015 Published, JBC Papers in Press, May 5, 2015, DOI 10.1074/jbc.M114.599399

Natasha M. Sosanya^द, Luisa P. Cacheaux^{‡1}, Emily R. Workman^{‡||}, Farr Niere^{‡2}, Nora I. Perrone-Bizzozero**, and Kimberly F. Raab-Graham \$\\$ \| \]

From the † Center for Learning and Memory, Department of Neuroscience, § Institute for Cell Biology, and $^{\parallel}$ Institute for Neuroscience, University of Texas, Austin, Texas 78712, [¶]United States Army Institute of Surgical Research, Joint Base San Antonio-Fort Sam, Houston, Texas 78234, and **Department of Neurosciences, Psychiatry and Behavioral Sciences, University of New Mexico Health Sciences Center, Albuquerque, New Mexico 87131

Background: Memory requires protein synthesis of dendritic CaMKII α .

Results: HuD directs CaMKIIα expression in a branch-specific manner. mTOR inhibition reduces HuD binding and promotes deadenylation of CaMKII α mRNA.

Conclusion: mTOR activity tags synapses, allowing HuD to capture CaMKII α in a branch-specific manner. Significance: mTOR and HuD provide a molecular model for the synaptic tagging and capture hypothesis.

The fate of a memory, whether stored or forgotten, is determined by the ability of an active or tagged synapse to undergo changes in synaptic efficacy requiring protein synthesis of plasticity-related proteins. A synapse can be tagged, but without the "capture" of plasticity-related proteins, it will not undergo long lasting forms of plasticity (synaptic tagging and capture hypothesis). What the "tag" is and how plasticity-related proteins are captured at tagged synapses are unknown. Ca2+/calmodulin-dependent protein kinase II α (CaMKII α) is critical in learning and memory and is synthesized locally in neuronal dendrites. The mechanistic (mammalian) target of rapamycin (mTOR) is a protein kinase that increases CaMKIIα protein expression; however, the mechanism and site of dendritic expression are unknown. Herein, we show that mTOR activity mediates the branch-specific expression of CaMKIIα, favoring one secondary, daughter branch over the other in a single neuron. mTOR inhibition decreased the dendritic levels of CaMKII α protein and mRNA by shortening its poly(A) tail. Overexpression of the RNA-stabilizing protein HuD increased CaMKII α protein levels and preserved its selective expression in one daughter branch over the other when mTOR was inhibited. Unexpectedly, deleting the third RNA recognition motif of HuD, the domain that binds the poly(A) tail, eliminated the branch-specific expression of CaMKII α when mTOR was active. These results provide a model for one molecular mechanism that may underlie the synaptic tagging and capture hypothesis where mTOR is the tag, preventing deadenylation of CaMKIIα mRNA, whereas HuD captures and promotes its expression in a branch-specific manner.

Activation of mTOR⁴ kinase is required for protein synthesisdependent, late phase long term potentiation (LTP) and memory consolidation (1, 2). mTOR consists of two subunits, mTORC1 and mTORC2. mTORC1, a serine/threonine kinase, promotes cap-dependent translation by phosphorylating p70 S6 kinase and eIF4E-binding protein (3). One notable mRNA whose translation is regulated by mTORC1 is Ca²⁺/calmodulindependent protein kinase II α (CaMKII α) (4, 5). CaMKII α is important for the induction and maintenance of LTP and memory (6). The importance of locally translated CaMKII α mRNA in memory consolidation was demonstrated in a mouse where the dendritic targeting sequence of CaMKII α in the genome was disrupted (7). Moreover, synapses that express protein synthesis-dependent LTP tend to occur on one dendritic daughter branch as opposed to the synapses of both daughter branches (8). Thus, further insight into the subcellular loci of CaMKIIα expression in dendrites may yield information regarding the importance of dendritic branches in memory formation.

The expression of the RNA-binding protein HuD is correlated with both spatial learning and contextual fear conditioning

^{*} This work was supported by National Science Foundation (NSF) Grants IOS 1026527 and IOS 1355158 (to K. F. R.-G.) and by National Institutes of Health Grants R01 NS30255 and DA034897 (to N. I. P.-B.). The authors declare that they have no conflicts of interest with the contents of this article.

¹ Supported by NSF Postdoctoral Research Fellowship in Biology DBI-1103738.

² Supported by NSF Postdoctoral Research Fellowship in Biology DBI-1306528.

³ To whom correspondence should be addressed: Center for Learning and Memory, Department of Neuroscience, University of Texas, 1 University Station, C7000, Austin, TX 78712. Tel.: 512-232-0892; E-mail: Kimberly@ mail.clm.utexas.edu.

⁴ The abbreviations used are: mTOR, mechanistic (mammalian) target of rapamycin; CaMKII α , Ca²⁺/calmodulin-dependent protein kinase II α ; RRM, RNA recognition motif; LTP, long term potentiation; mTORC, mTOR complex; eGFP, enhanced GFP; DIV, days in vitro; Rapa, rapamycin; AP5, (2R)amino-5-phosphonovaleric acid; DMSO, dimethyl sulfoxide; P-S6, phospho-S6; FISH, fluorescence in situ hybridization; BVI, branch variability index; myr-dGFP, myristoylated destabilized GFP; NMDAR, NMDA receptor; KD, knockdown; ANOVA, analysis of variance.

(9-11). Furthermore, expression of several HuD target mRNAs is associated with improved cognition (9, 12, 13). Recently, we determined that mTORC1 kinase serves as a switch for translation of specific mRNAs such as CaMKII α through HuD. We demonstrated that when mTORC1 is active HuD binds to its high affinity target mRNAs including CaMKII α , stabilizing the mRNA and promoting its translation. When mTORC1 is inhibited, CaMKII α mRNA is degraded, thus releasing HuD and allowing it to bind to low affinity target mRNAs such as the voltage-gated potassium channel Kv1.1 (5). How CaMKII α mRNA is degraded is unclear. Collectively, these data strongly support a role for mTOR activity and HuD to promote the translation of mRNAs that support learning and memory.

The synaptic tagging and capture hypothesis proposes that the synapses activated during early LTP become tagged in a protein synthesis-independent manner (14). For the tagged synapse to undergo lasting changes in synaptic efficacy, it must capture plasticity-related proteins or the mRNAs that code for these proteins (15). The requirement for protein synthesis comes from studies that demonstrate that the conversion of early LTP to late phase LTP is blocked with the addition of protein synthesis inhibitors such as the mTORC1 inhibitor rapamycin (16, 17). Although a great deal is known about global mTORC1-regulated translation, it is unknown whether mTORC1 regulates protein expression in a site-specific manner. In this study, we demonstrate an unexpected role for HuD in mTORC1-regulated branch-specific CaMKIIα protein expression. Using immunocytochemistry and in situ hybridization to map $CaMKII\alpha$ protein and mRNA, we show that CaMKII α is preferentially expressed in one daughter branch versus the other when mTORC1 is active, suggesting that mTORC1 serves as a tag for CaMKII α expression.

We determined that HuD mediates the branch-specific expression of CaMKII α likely through the binding of its poly(A) tail. Furthermore, we found that HuD expression is branch-specific and that this process does not rely on mTORC1 activity. Thus, our findings provide a model in which mTORC1 activity and the branch-specific targeting of HuD determine which mRNAs are available to be translated and in turn the propensity of a dendritic branch to undergo site-specific and long lasting forms of plasticity.

Experimental Procedures

Transfection and Immunocytochemistry—Neurons were cultured as described previously in Sosanya *et al.* (5). Briefly, hippocampi from E18–19 rats were collected, dissociated, and plated. Neurons were plated at a density of 50,000 neurons/12-mm coverslip. Cultured hippocampal neurons were transfected with pcDNA+eGFP, pcHuD+eGFP, and pcHuD I+II+eGPF at 17–20 days *in vitro* (DIV) using Lipofectamine 2000 (Life Technologies) as described by the manufacturer using Neurobasal medium (Life Technologies). Cloning of pcHuD and pcHuD I+II is described in Anderson *et al.* (18). At DIV 21–24, 4 days post-transfection, neurons were treated with 200 nM rapamycin, 100 μ M (2R)-amino-5-phosphonovaleric acid (AP5), DMSO (vehicle for Rapa), or H₂O (vehicle for AP5) for 75 min. Following treatment, neurons were fixed for 20 min at room temperature in 4% paraformaldehyde followed by three

washes in $1\times$ phosphate-buffered saline (PBS). Neurons were then permeabilized for 5 min with 0.25% Triton in $1\times$ PBS (Sigma) and blocked for 1 h in blocking solution (8% goat serum, 0.25% Triton, $1\times$ PBS) at room temperature. Primary antibodies were incubated overnight at 4 °C in blocking solution followed by secondary antibody incubation for 1 h at room temperature in blocking solution. The cells were then washed (PBS), mounted (Fluoromount-G, SouthernBiotech), and imaged.

Antibodies—Primary antibodies used were: mouse anti-CaMKII α (1:200; LifeSpan Biosciences), chicken anti-GFP (1:200; Aves Labs), mouse anti-Kv1.1 extracellular (Neuromab), rabbit anti-myc (1:200, Sigma), rabbit anti-phospho-S6 (P-S6) (1:50; Cell Signaling Technology), and chicken anti-MAP2 (1:2000; Abcam). Secondary antibodies from Life Technologies used at 1:400 were Alexa Fluor 488 anti-chicken, Alexa Fluor 555 anti-mouse, and Alexa Fluor 647 anti-rabbit.

Fluorescence in Situ Hybridization (FISH)—For CaMKIIα or HuD mRNA detection, fluorescence in situ hybridization was conducted using the ViewRNA ISH Cell Assay kit (Affymetrix) as described in Cajigas *et al.* (19). The CaMKII α and HuD probe sets were designed commercially by Affymetrix. Briefly, primary hippocampal neurons (DIV 20-21) were fixed at room temperature for 30 min with a 4% paraformaldehyde solution (4% paraformaldehyde, 5.4% glucose, 0.01 M sodium metaperiodate in lysine-phosphate buffer). Proteinase K treatment was omitted, and the rest of the hybridization was completed according to the manufacturer's instructions. The cells were then washed with PBS and blocked with 4% goat serum in PBS for 1 h followed by incubation in primary antibody (chicken anti-MAP2 or chicken anti-GFP) overnight at 4 °C. After three washes with PBS, the cells were incubated with the appropriate secondary antibody for 1 h at room temperature and washed with PBS. The coverslips were then mounted with an antifading mounting medium and imaged as described above.

Quantification of Phospho-S6 Puncta and CaMKIIa mRNA Puncta-Images were acquired using a Leica SP5 confocal microscope (63× objective lens; numerical aperture, 1.2) with sequential scanning. Series of z-stacks were collected at 0.5-µm intervals for a total of 5.0 µm. Dendrites were chosen blindly based on MAP2 or eGFP signal. Following image acquisition, a binary mask of equally thresholded images was created using Meta Imaging Series 7.8. To measure branch variability, $10-\mu$ m-long regions of interest were drawn before and after the primary branch point of the MAP2 or eGFP dendrite as described by Govindarajan et al. (8). P-S6 punctum intensity in the primary and secondary branches and CaMKII α punctum intensity in the cell body and primary and secondary branches were measured using integrated morphometry image analysis. P-S6 intensity in the cell body was taken as a ratio over eGFP or MAP2 as the signal was not punctate in the cell body. Individual puncta were counted in the primary and secondary branches similar to Cajigas et al. (19). To determine whether mTOR was equally or differentially active between daughter branches, the number of P-S6 puncta/10- μ m area after the branch point was determined for each daughter branch emerging from a single parent dendrite. The absolute value of the difference in punc-

tum number per 10 µm area between the arbitrarily assigned daughter branch A and daughter branch B was determined.

Image Analysis, Branch Variability Index (BVI), and Threedimensional Rendering-Following image acquisition as described above, the ratio of CaMKIIα, Kv1.1, or myc-HuD over eGFP signal (volume control) was determined by the ImageJ plug-in Ratio Regions of Interest (ROI) Manager under Stacks-T-Functions. Daughter branches emerging from a single parent dendrite were arbitrarily assigned A and B (see Fig. 1A). To avoid negative numbers, we used the absolute value of branch A minus B. BVI was calculated by the following equation: BVI = |Daughter branch A - Daughter branch B|/AverageBVI of control neurons for their individual culture. Three-dimensional rendering was achieved using the ImageJ plug-in Interactive 3D Surface Plot.

Poly(A) Tail Length Assay—The poly(A) tail length assay was carried out according to Wuetal. (21) and similarly to Udagawa et al. (20). Cultured cortical neurons between DIV 21 and 28 were treated in artificial cerebrospinal fluid for 10 min for time point 0 or rapamycin for 60, 90, or 180 min. Neurons were harvested in HB buffer B (20 mm HEPES, pH 7.4, 5 mm EDTA, pH 8.0 with RNaseOut and tris(2-carboxyethyl)phosphine) and homogenized. Following a low speed spin (900 rpm for 10 min), total RNA was isolated using Tri-LS following the manufacturer's protocol (Applied Biosystems). Reverse transcription was performed with the anchor-oligo(dT) primer (5'-GCG-AGCTCCGCGGCCGCGT-3') using the Superscript III first strand cDNA synthesis kit (Life Technologies). Subsequent PCR was performed with 100 ng of cDNA using AmpliTaq Gold DNA polymerase (Applied Biosystems) with specific CaMKIIα forward (5'-CCGAAGCTTCTCTCTTTT-TTTATTATGTGGCTGTG-3'; oligo 1) and reverse (5'-GCT-CTAGACACATAAATTTGTAGCTATTTATTCC-3') oligos or Kv1.1 forward (5'-GCCGCCGCAGCTCCTACTATCA-G-3'; oligo 1) and reverse (5'-GCTTTTGATTGCTTGCCTG-GTGCTT-3') oligos (13, 14). To detect the poly(A) tail, oligo 1 for CaMKII α or Kv1.1 was used in combination with the anchor-oligo(dT) primer. PCR was done with an initial denaturation step (95 °C for 5 min) followed by 10 cycles of 15 s at 95 °C, 15 s at 45 °C, and 1 min at 72 °C; then 50 cycles of 15 s at 95 °C, 15 s at 58 °C, and 1 min at 72 °C; and finally 7 min at 72 °C. The PCR products were resolved in a 2% agarose gel. As a control for the poly(A) tail length assay, 600 ng of total RNA was treated with RNase H and oligo(dT) for 20 min at 37 °C prior to RT-PCR.

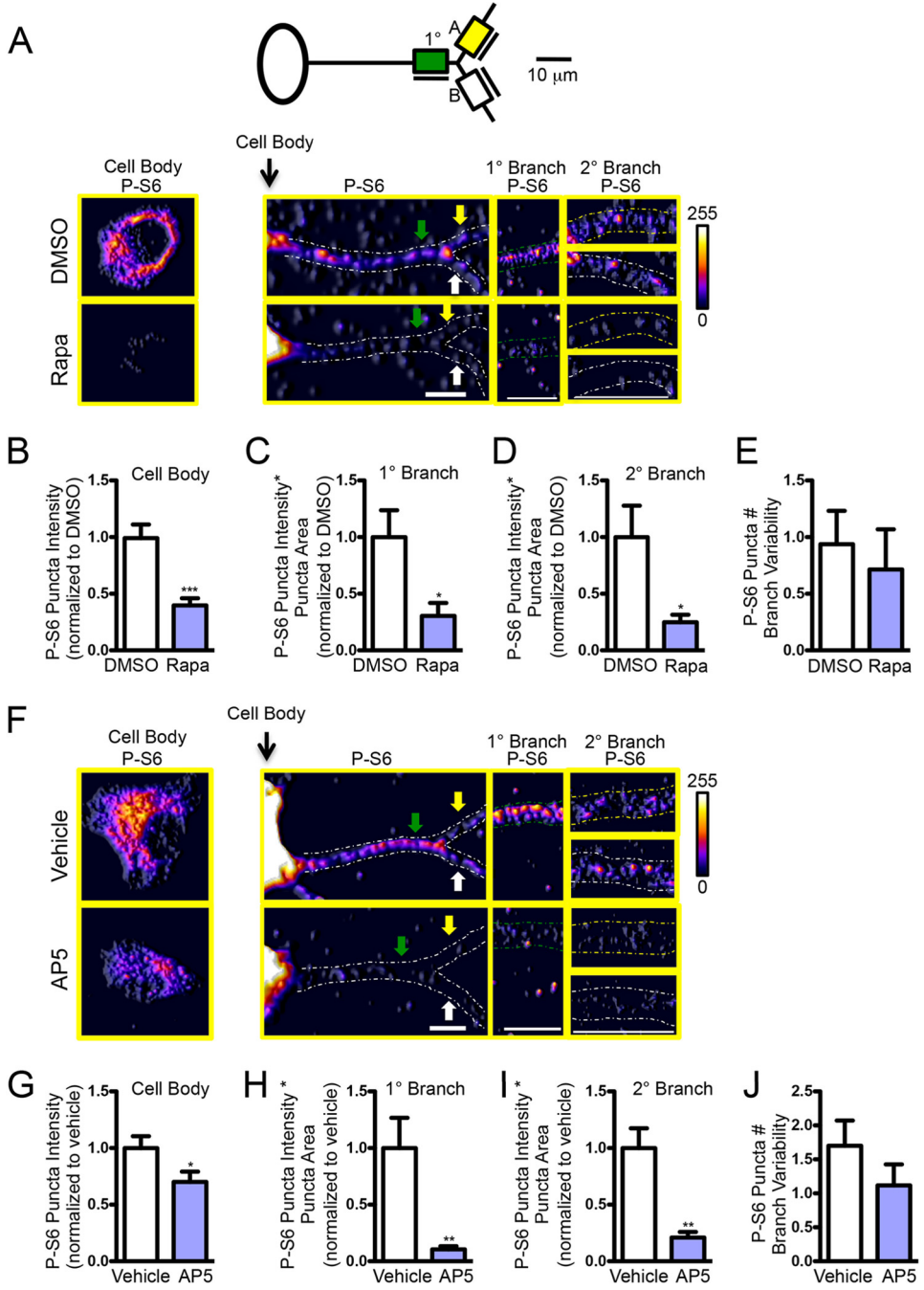
Knockdown of HuD with Short Hairpin RNA (shRNA)—For shRNA-mediated knockdown of HuD, primary hippocampal neurons were transfected on DIV 17 with peGFP and either plasmid (CGCATCCTGGTTGATpRetro-shHuD CAAGT) (22) or the pRetro control plasmid. The transfection protocol is described above. After 72 h, the cells were fixed and prepared for either CaMKIIα immunocytochemical analysis or HuD FISH.

Local Translation of Myristoylated Destabilized GFP (myrdGFP)-CaMKIIα UTR—Detailed methods regarding the detection of local translation of the coding sequence for a myristoylated, destabilized GFP flanked by the 5'- and 3'-untranslated regions of α -CAMKII have been reported by Aakalu *et al.* (23)

and Sutton et al. (24). In brief, fluorescence recovery after bleaching-live imaging of new CaMKII α translation using the myr-dGFP reporter was performed 36 h post-transfection with either myr-dGFP-CaMKIIα UTR HuD or myr-dGFP-CaMKII α UTR Δ HuD and dsRED. Neurons were live imaged in HEPES-based artificial cerebrospinal fluid using a 20× immersion lens on a Leica SP5 spinning disk confocal microscope. An initial z-stack of the full extent of the neuron was acquired. The dGFP signal was then bleached by acquiring one frame/s with a 488 nm argon laser set at full power for 100 frames. Following this, a z-stack of each neuron was then acquired approximately every 6 min for 30 min. The average change in green fluorescence was calculated at time t = 0 ($^{\text{F}}_{0}$), t = 6 (F_{6}), t = 12 (F_{12}), $t = 18 (F_{18})$, and $t = 30 (F_{30})$ for the same regions of interest 10 µm before and after each branch point. The percentage of change in green fluorescence ($\Delta F/F$) was calculated as ($(F_{30} - F)$) F_0)/ F_0) at 30-min postbleach. A similar equation was used for F_6 , F_{12} , and F_{18} . The BVI was calculated at t = 30 min as the absolute difference between the percentages of change in fluorescence for each daughter branch: $(\Delta F/F_A - \Delta F/F_B)$.

Results

NMDAR Signaling Activates mTORC1 in Cultured Hippocampal Neurons-For synapses to be tagged, they must be stimulated by synaptic activity, usually requiring N-methyl-Daspartate (NMDA) receptor activation. Using a simplified system, we have shown previously that NMDAR activity promotes the phosphorylation of mTORC1, and acute rapamycin treatment reduces it in cultured hippocampal and cortical neurons (21-28 DIV) (25). However, the subcellular localization of mTORC1 activity has not been determined. To this end, we treated neurons with vehicle, AP5, or the mTORC1 inhibitor rapamycin and stained for the downstream marker of active mTORC1, P-S6, a key ribosomal protein. Thus, we predict that during elevated spontaneous NMDAR activity, such that occurs in dissociated neurons after several weeks in culture (14), mTORC1 will be active throughout the dendritic arbor (Fig. 1A). As expected, mTORC1 was strongly activated in the cell body (Fig. 1B) and primary and secondary branches (Fig. 1, C and D) of cultured primary hippocampal neurons as indicated by the change in signal intensity of P-S6 puncta or hot spots with rapamycin. To determine whether mTORC1 activity is equally or differentially stimulated between two daughter branches that emerge from a single parent dendrite, we counted the number of P-S6 hot spots/10-µm area directly after the branch point similar to Govindarajan et al. (8). We arbitrarily assigned one daughter branch A and the other B (Fig. 1A, schematic, yellow and white boxes). We then took the absolute value of the difference in P-S6 hot spots between branches A and B. As predicted, there was relatively little difference between the two daughter branches, only differing in P-S6 punctum number by ~ 1 hot spot when mTORC1 was active (branch with most puncta averaged \sim 3 \pm 0.24 *versus* the branch with the fewest number of puncta averaging \sim 2 \pm 0.41). Notably, the signal intensity of the P-S6 hot spots was significantly reduced with mTORC1 inhibition; however, the remaining signal between branches was relatively the same (Fig. 1E; BVI for DMSO,



 $FIGURE\ 1.\ \textbf{NMDAR signaling leads to mTORC1 activity throughout the dendritic arbor.} \textit{A}, schematic of neuron (top) shows where punctum signal intensity throughout the dendritic arbor.} \textit{A}, schematic of neuron (top) shows where punctum signal intensity throughout the dendritic arbor.} \textit{A}, schematic of neuron (top) shows where punctum signal intensity throughout the dendritic arbor.} \textit{A}, schematic of neuron (top) shows where punctum signal intensity throughout the dendritic arbor.} \textit{A}, schematic of neuron (top) shows where punctum signal intensity throughout the dendritic arbor.} \textit{A}, schematic of neuron (top) shows where punctum signal intensity throughout the dendritic arbor.} \textit{A}, schematic of neuron (top) shows where punctum signal intensity throughout the dendritic arbor.} \textit{A}, schematic of neuron (top) shows where punctum signal intensity throughout the dendritic arbor.} \textit{A}, schematic of neuron (top) shows where punctum signal intensity throughout the dendritic arbor.} \textit{A}, schematic of neuron (top) shows where punctum signal intensity throughout the dendritic arbor.} \textit{A}, schematic of neuron (top) shows where punctum signal intensity throughout the dendritic arbor.} \textit{A}, schematic of neuron (top) shows where punctum signal intensity throughout the dendritic arbor.} \textit{A}, schematic of neuron (top) shows where the dendritic arbor.} \textit{A}, schematic of neuron (top) shows where the dendritic arbor.} \textit{A}, schematic of neuron (top) shows where the dendritic arbor.} \textit{A}, schematic of neuron (top) shows where the dendritic arbor.} \textit{A}, schematic of neuron (top) shows where the dendritic arbor.} \textit{A}, schematic of neuron (top) shows where the dendritic arbor.} \textit{A}, schematic of neuron (top) shows where the dendritic arbor.} \textit{A}, schematic of neuron (top) shows where the dendritic arbor.} \textit{A}, schematic of neuron (top) shows where the dendritic arbor.} \textit{A}, schematic of neuron (top) shows where the dendritic arbor.} \textit{A}, schematic of neuron (top) shows where the dendritic arbor.} \textit{A},$ measurements were taken for quantitative analysis throughout all figures. Boxed regions (primary branch, green; daughter branch A, yellow; daughter branch B, white) represent 10-µm segments prior to and after the branch point used for analysis. Immunostaining of P-S6 hot spots in DMSO (carrier)- and rapamycin (200 nm)-treated cultured hippocampal neurons. Cell body images were taken with a lower gain relative to dendrites to avoid saturation of signal (left). MAP2 expression (not shown) was used to outline the dendrites of the representative neurons. Colored arrows refer to the corresponding blown up region of the dendrite that is outlined with the dotted line in the same color to the right. Images were pseudocolored, and three-dimensional rendering was achieved using the Interactive 3D Surface Plot plug-in in ImageJ to demonstrate differences in signal intensity. Scale bar, 10 μ m. B, P-S6 punctum signal intensity was measured in the cell body and normalized by area for DMSO- and rapamycin-treated neurons. Note that P-S6 punctum intensity decreases with rapamycin treatment in the cell body. *, p < 0.05 by unpaired Student's t test. DMSO, p = 11 neurons; Rapa, p = 12 neurons. C, P-S6 punctum signal intensity was measured in a region 10 μ m before the primary branch point of DMSO- and rapamycin-treated neurons. DMSO, n=13 primary dendrites; Rapa, n=17 primary dendrites. D, P-S6 punctum signal intensity was measured in a region 10 μ m after the primary branch point of DMSO-and rapamycin-treated neurons. *, p < 0.05 by unpaired Student's t test. DMSO, n = 26 secondary branches; Rapa, n = 24 secondary branches. E, change in mTORC1 activity between daughter branches was determined by counting the number of P-S6 puncta in each daughter branch/ 10° - μ m area after each branch point and using the following equation: Δ P-S6 hot spots = |Daughter branch A/Area - Daughter branch B|. DMSO, n = 16 daughter branch pairs; Rapa, n = 14 daughter branch pairs. F-J, cultured hippocampal neurons were treated with vehicle (H₂O) or AP5 (100 μ M) and immunostained for P-S6 puncta. MAP2 (not shown) expression was used to outline the dendrites of the representative neurons. Quantification was performed on non-saturated images of cell bodies. Quantification of P-S6 puncta was performed as described above for the rapamycin treatment. Images were pseudocolored, and three-dimensional rendering was achieved using the Interactive 3D Surface Plot plug-in in ImageJ. * in y axis in H indicates multiplication. Scale bar, 10 μ m. Vehicle, n = 19 cell bodies, 19 primary (1°) branches, 39 secondary (2°) branches, and 20 paired daughter branches; AP5, n = 16 cell bodies, 18 primary branches, 31 secondary branches, and 17 paired daughter branches. **, p < 0.01 by unpaired Student's t test. Error bars represent S.E.

 0.94 ± 0.30 ; BVI for Rapa, 0.71 ± 0.35 ; single t test not significantly different from zero).

In contrast to rapamycin, blocking NMDAR signaling with AP5 had a smaller effect of \sim 30% *versus* a \sim 60% reduction of the P-S6 signal in the cell body (Fig. 1, A and B and F and G). Interestingly, AP5 significantly reduced the signal intensity of P-S6 in the primary, parent dendrite by \sim 90% (Fig. 1H; vehicle (water), 1 ± 0.27 ; AP5, 0.10 ± 0.03) and the secondary branch by \sim 79% (Fig. 1, F and I; vehicle (water), 1.00 ± 0.17 ; AP5, 0.21 ± 0.05). Similar to rapamycin, the number of detectable puncta did not change between daughter branches (Fig. 1, E and I). These data suggest that NMDAR activity stimulates mTORC1 throughout the dendritic arbor and can be specifically blocked with either AP5 or rapamycin treatment.

NMDAR and mTORC1 Activity Is Required for CaMKIIa Branch-specific Expression—NMDAR activation stimulates the mTOR-dependent, local protein synthesis of CaMKII α mRNA (4). However, it is unknown whether mTORC1 differentially regulates CaMKIIα protein expression in one daughter branch over the other. To answer this question, we determined whether CaMKIIα protein expression was branch-specific using immunofluorescence with blockers of NMDAR/ mTORC1 activity. eGFP expression allowed us to clearly visualize individual neurons and normalize signal by volume. Although the cell body CaMKII α signal in neurons was highly variable, NMDAR inhibition with AP5 but not mTORC1 inhibition with rapamycin reduced CaMKIIα protein expression dramatically by \sim 66% (Fig. 2, A and B and F and G). These results suggest that $CaMKII\alpha$ expression in the cell body may be independent of mTORC1 activity.

Next, we measured CaMKII α in the dendrites by determining the average signal intensity in the primary apical dendrite prior to the first branch and normalized by eGFP as a volume control (Fig. 2, A, C, F, and H). Inhibition of mTORC1 by rapamycin (Fig. 2, A and C) or NMDARs by AP5 (Fig. 2, F and H) reduced the dendritic expression of CaMKII α in the primary parent branch by \sim 50 and 40%, respectively (Fig. 2C: DMSO, 1.00 ± 0.22 ; Rapa, 0.49 ± 0.05 ; Fig. 2G: vehicle, 1.00 ± 0.15 ; AP5, 0.60 \pm 0.10). Next, we measured the average signal intensity of CaMKIIα in each daughter branch 10 μm from the branch point normalized by eGFP. Again, reducing mTORC1 activity either by NMDAR antagonism (AP5) or rapamycin decreased the overall expression of CaMKII α in the secondary branches (Fig. 2, A, D, F, and I). To determine whether CaMKII α was differentially expressed between daughter branches, we determined its BVI by measuring the signal intensity of CaMKIIα normalized to eGFP for each daughter branch and then took the absolute value of paired daughter branch A minus daughter branch B. This difference was divided by the average BVI for control neurons. In this case, a value of 0 indicates that the protein is equally distributed between daughter branches (see "Experimental Procedures" for the equation). As the BVI moves away from 0, protein expression becomes more polarized in one daughter branch over the other. Indeed, CaMKII α protein was enriched in one daughter branch by at least ~2-fold when mTORC1 was active relative to neurons treated with AP5 or the mTORC1 inhibitor rapamycin (Fig. 2E: BVI for DMSO, 1.00 \pm 0.06; BVI for Rapa, 0.45 \pm 0.07; Fig. 2*J*: BVI for vehicle, 1.00 \pm 0.27; BVI for AP5, 0.24 \pm 0.09).

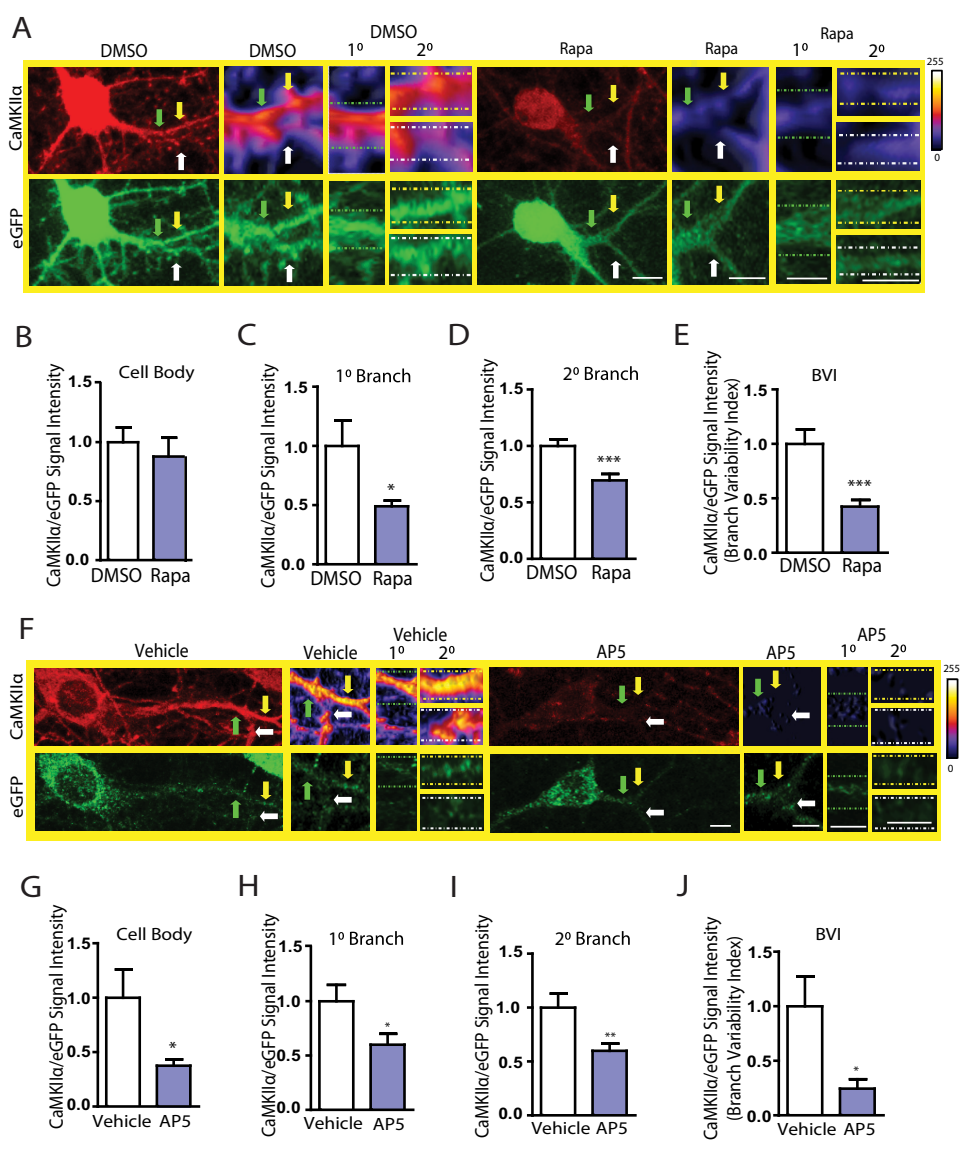
Branch-specific Expression of Kv1.1 Does Not Require mTORC1 Activity—To determine whether branch-specific expression is generally dependent on mTORC1, we examined the expression of Kv1.1 protein whose dendritic expression is negatively regulated by mTORC1 activity. As observed previously (5, 25, 26), mTORC1 inhibition increased Kv1.1 protein \sim 100% in the primary and \sim 70% in the secondary dendrites (primary dendrite: DMSO, 1.00 ± 0.17 ; Rapa, 2.04 ± 0.45 ; secondary dendrite: DMSO, 1.00 ± 0.13 ; Rapa, 1.72 ± 0.27 ; Fig. 3, A-D). Although we did not observe changes in BVI when mTORC1 activity was disrupted, the BVI of ~1 suggests that Kv1.1 protein expression was more abundant in one daughter branch over the other under both conditions (Fig. 3*E*). These results altogether suggest that both CaMKII α and Kv1.1 expression is branch-specific, favoring one daughter branch over the other in a single neuron. In contrast, mTORC1 activity regulates the drop in the branch-specific expression of CaMKII α but not of Kv1.1.

CaMKII\alpha mRNA Targets One Daughter Branch over the Other in a Single Neuron When mTORC1 Is Active—An unresolved debate concerning the synaptic tagging and capture hypothesis is whether it is the mRNA or protein that is "captured" in a site-specific manner. Although CaMKII α protein is branch-specific (Fig. 2), it is unclear whether the mRNA is as well. To answer this question, we performed FISH against CaMKIIα mRNA when mTORC1 was active or inhibited with rapamycin. Control and rapamycin-treated neurons were probed for CaMKII α mRNA and quantified (Fig. 4A). As a negative control, we used a sense probe that did not detect any signal (Fig. 4B). Consistent with CaMKII α protein levels, there was no change in the number of mRNA granules in the cell body when normalized by area (Fig. 4, A and C). In contrast, there was a significant reduction in total CaMKIIα-positive mRNA granules in the primary and secondary dendritic branches of rapamycin-treated neurons (Fig. 4, D and E).

To determine whether the mRNA targets one branch over the other, we determined whether there were more CaMKIIlphamRNA-positive granules in one daughter branch over the other in a single neuron. As expected, we detected a range between \sim 4 (high branch) and \sim 1 (low branch), with \sim 3 more granules per 10- μ m segment that were selectively targeted to one branch over the other (Fig. 4F) when mTORC1 was active (Fig. 4F; DMSO, 2.5 \pm 0.28; Rapa, 0.65 \pm 0.15). As seen with the protein, the number of mRNA-positive granules was decreased with rapamycin, reducing the branch-selective expression of CaMKII α mRNA. Of note, the signal intensity of the granules that remained present after rapamycin treatment is relatively equal to the signal intensity of those that were present when mTORC1 was active (Fig. 4G). Consistent with the branch-selective expression of CaMKIIα protein, these results suggest that when mTORC1 is active CaMKIIα mRNA localizes to one daughter branch over the other within a single neuron.

mTORC1 Inhibition Results in the Rapid Degradation of CaMKIIα mRNA by Shortening of the Poly(A) Tail—In light of these data, two questions remain unanswered: 1) what mediates





 $FIGURE\ 2.\ \textbf{NMDAR}\ and\ \textbf{mTORC1}\ activity\ \textbf{lead}\ \textbf{to}\ \textbf{branch-specific}\ \textbf{expression}\ \textbf{of}\ \textbf{CaMKII}\alpha\ \textbf{protein}\ \textbf{levels}\ \textbf{that}\ \textbf{is}\ \textbf{reduced}\ \textbf{with}\ \textbf{NMDAR/mTORC1}\ \textbf{blockade.}$ A, eGFP-expressing cultured hippocampal neurons were treated with DMSO or rapamycin and immunostained for CaMKII α . Representative neurons are shown. Colored arrows refer to the corresponding blown up region of the dendrite that is outlined with the dotted line in the same color to the right. CaMKII α images were pseudocolored, and three-dimensional rendering was achieved using the Interactive 3D Surface Plot plug-in in ImageJ to demonstrate differences in signal intensity. Scale bar, 10 μ m. B, the signal intensity of CaMKII α in the cell body of neurons treated with DMSO or rapamycin was measured as a ratio over eGFP. Only unsaturated cell bodies were used for the quantification. DMSO, n = 18 neuronal cell bodies; Rapa, n = 13 neuronal cell bodies. C and D, the signal intensity of CaMKII α in neurons treated with DMSO or rapamycin was measured as a ratio over eGFP. Note that CaMKII α protein decreases with rapamycin treatment. *, p < 0.05; ***, p < 0.005 by unpaired Student's t test. Primary (1°) branch: DMSO, n = 21; Rapa, n = 24; secondary (2°) branch: DMSO, n = 2172; Rapa, n = 71. E, BVI was determined by normalizing all signals by eGFP within the same branch and using the following equation: BVI = |Daughter branch|Daughter branch B/Averaged control BVI. Note that CaMKII α BVI is reduced when mTORC1 is inhibited with rapamycin. ***, p < 0.005 by unpaired Student's t test. CaMKII α : DMSO, n=33 paired daughter branches; Rapa, n=29 paired daughter branches. F, eGFP-expressing cultured hippocampal neurons were treated with vehicle or AP5 and immunostained for CaMKIIa. Representative neurons are shown. CaMKIIa images were also pseudocolored, and three-dimensional rendering was achieved using the Interactive 3D Surface Plot plug-in in ImageJ. Scale bar, 10 μ m. G, the signal intensity of CaMKII α in the cell body of neurons treated with vehicle or AP5 was measured as a ratio over eGFP. Vehicle, n = 16 neuronal cell bodies; AP5, n = 14 neuronal cell bodies. H, the signal intensity of CaMKII α in neurons treated with vehicle or AP5 was measured as a ratio over eGFP 10 μ m before the branch point. Note that CaMKII α protein decreases with AP5 treatment. *, p < 0.05 by unpaired Student's t test. Vehicle, n = 14 primary branches; AP5, n = 12 primary branches. l, the signal intensity of CaMKII α in neurons treated with vehicle or AP5 was measured as a ratio over eGFP 10 μ m after the branch point. **, p < 0.01 by unpaired Student's t test. Vehicle, n = 28 branches; AP5, n = 26 branches. J, BVI was determined by normalizing all signals by eGFP within the same branch and using the following equation: BVI = |Daughter branch A - Daughter branch B|/Averaged control BVI. Note that CaMKII\alpha BVI is reduced when NMDAR is inhibited with AP5. *, p < 0.05 by unpaired Student's t test. Vehicle, n = 14 paired daughter branches; AP5, n = 11 paired daughter branches. Error bars represent S.E.

the branch-specific targeting of CaMKII α mRNA and 2) how does inhibition of mTORC1 reduce it? By first determining the mechanism that reduces branch-specific mRNA targeting, we might glean insight into the factors that mediate the process. In yeast, inhibition of TORC1 accelerates the deadenylation-decapping pathway (27). mRNAs that decay rapidly in the pres-

ence of rapamycin have shorter poly(A) tails possibly through rapid deadenylation (27). Thus, we hypothesized that deadenylation of CaMKII α mRNA underlies the reduced CaMKII α mRNA when mTORC1 is inhibited. Using the poly(A) tail length assay, we measured CaMKII α mRNA poly(A) tail length when mTORC1 kinase was active or inhibited by rapamycin.

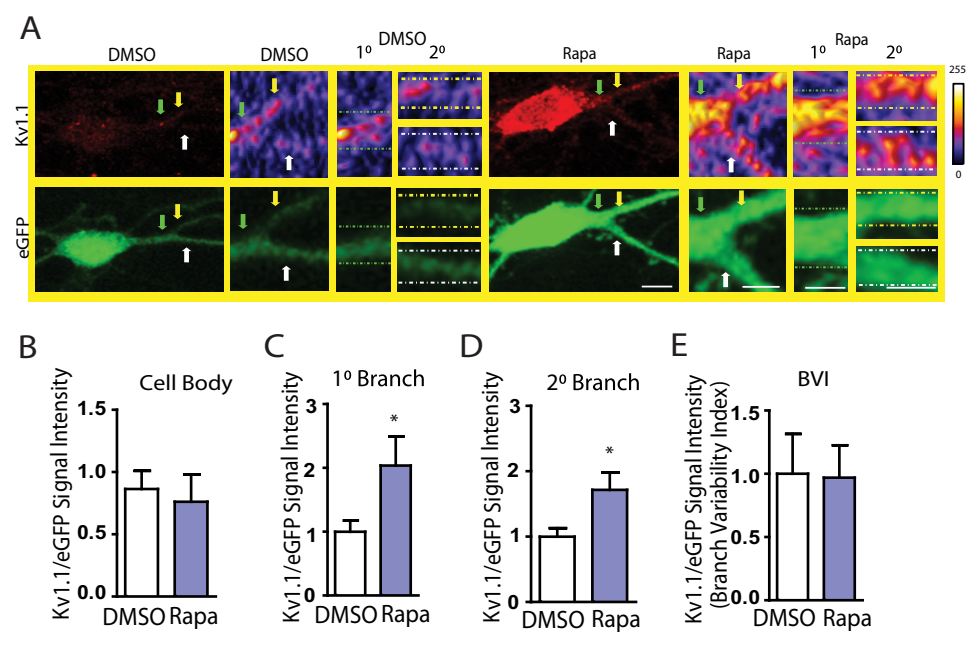


FIGURE 3. **Branch-specific expression of Kv1.1 does not require mTORC1 activity.** *A*, representative images of neurons treated with DMSO (control) or rapamycin and immunostained for Kv1.1. *Colored arrows* refer to the corresponding blown up region of the dendrite that is *outlined* with the *dotted line* in the same color to the *right*. Note that the dendritic expression of Kv1.1 increases with mTORC1 inhibition. Kv1.1 images were also pseudocolored, and three-dimensional rendering was achieved using the Interactive 3D Surface Plot plug-in in ImageJ to demonstrate change in signal intensity. *Scale bar*, 10 μ m. *B–D*, quantification of Kv1.1 signal intensity normalized by eGFP in the cell body (*B*) as well as the primary (1°) (*C*) and secondary (2°) dendrites (*D*). The signal intensity of Kv1.1 in neurons treated with DMSO or rapamycin was measured as a ratio over eGFP 10 μ m before or after the branch point. *, p < 0.05 by unpaired Student's t test. Cell body: DMSO, n = 11; Rapa, n = 9; primary branch: DMSO, n = 11; Rapa, n = 9; secondary branch: DMSO, n = 24; Rapa, n = 18. *E*, BVI was determined by normalizing all signals by eGFP within the same branch and using the following equation: BVI = |Daughter branch A - Daughter branch B|/Averaged control BVI. Note that Kv1.1 expression in secondary dendrites is polarized in both control and rapamycin-treated neurons. Kv1.1: DMSO, n = 12 paired daughter branches; Rapa, n = 9 paired daughter branches. *Error bars* represent S.E.

The reduction in poly(A) tail length, band intensity (Fig. 5*A*), and sensitivity to RNase H treatment (Fig. 5*B*) all indicate that inhibiting mTORC1 activity shortens the CaMKII α mRNA poly(A) tail. Notably, Kv1.1 mRNA levels remained roughly the same (5), whereas the poly(A) tail length remained relatively the same with mTORC1 inhibition (Fig. 5*C*). These results favor the hypothesis that the mTORC1-dependent reduction in CaMKII α mRNA is mediated by its rapid deadenylation and subsequent mRNA degradation.

The Binding of the RNA-binding Protein HuD to the 3'-UTR of CaMKII\alpha Is Required for Its Branch-selective Expression— Because the branch-specific expression of Kv1.1 was not affected by mTORC1 activity, we considered the possibility that HuD, an RNA-binding protein that binds to both mRNAs, could mediate branch-specific expression of CaMKII α . We recently demonstrated that HuD/CaMKIIα mRNA interaction mediates the mTORC1-dependent expression of CaMKII α protein (5). Furthermore, we showed that CaMKIIα mRNA and Kv1.1 mRNA compete for HuD binding with CaMKII α mRNA "winning" when mTORC1 is active due to the higher affinity for HuD and abundance of CaMKII α (5). In agreement with our data suggesting that reduced mTORC1 activity leads to the shortening of the CaMKIIα mRNA poly(A) tail (Fig. 5), HuD stabilized its target mRNAs by delaying the onset of mRNA degradation and had an ~10-fold higher affinity for mRNAs with long poly(A) tails (>150 nucleotides) (18, 28, 29). Thus, if HuD is required for the branch-selective expression of CaMKII α , then we would predict that deletion of HuD binding sites from the 3'-UTR of CaMKIIα would eliminate the polarized expression of CaMKII α . Because CaMKII α mRNA has 35 HuD binding sites (30), we turned to a reporter construct coding for myr-dGFP fused to the dendritic targeting sequence within the 3′-UTR of CaMKII α that contains eight overlapping HuD binding sites (5, 23). As expected, neurons that expressed this reporter construct showed selective expression of myr-dGFP in one daughter branch over the other, having a BVI of \sim 1 (Fig. 6, A and B). In contrast, when we expressed this reporter construct with the HuD binding sites removed, the myr-dGFP signal seemed to accumulate at the branch point, reducing the BVI by 55% (Fig. 6, A and B; myr-dGFP-CaMKII α UTR, 1.00 \pm 0.19; myr-dGFP-CaMKII α UTR Δ HuD, 0.45 \pm 0.13). These results suggest that HuD mediates the branch-selective expression of CaMKII α mRNA.

Knockdown of Endogenous HuD Reduces the Branch-selective Expression of CaMKII α —As a further test to assess the relative importance of HuD in mediating the branch-specific expression of CaMKII α in neurons, we transfected neurons with an shRNA designed and characterized to reduce or knock down (KD) HuD mRNA expression (22). To verify that the shRNA was effective at reducing HuD mRNA expression, we performed fluorescence in situ hybridization using an antisense probe set specific for HuD mRNA. As expected, only neurons transfected with eGFP and the HuD shRNA showed reduced HuD mRNA in the cell body (Fig. 7A, right panel, white arrow indicating nontransfected cells versus outlined transfected cell body). Furthermore, HuD mRNA was reduced by \sim 66% 72 h post-transfection in HuD KD neurons when compared with eGFP-expressing neurons that were transfected with vector

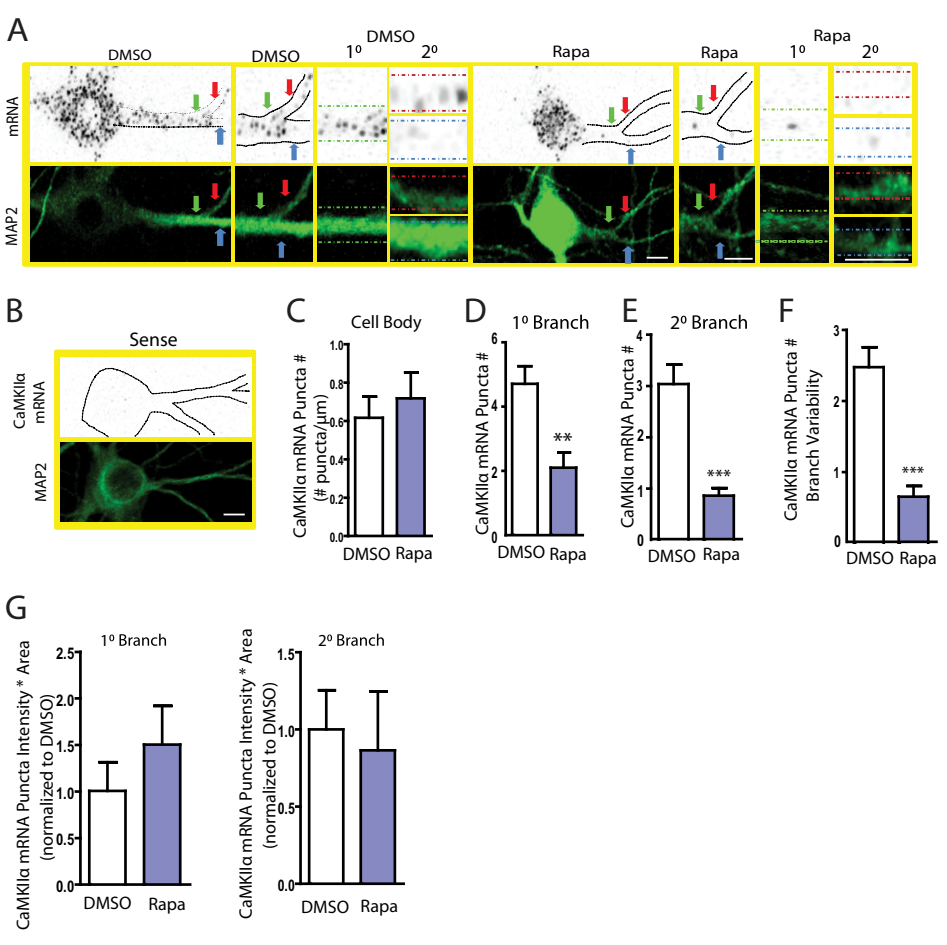


FIGURE 4. **mTORC1 activity leads to branch-specific expression of CaMKII** α mRNA that is reduced with mTORC1 inhibition. *A*, FISH using the CaMKII α mRNA-specific antisense probe. eGFP staining was used to outline the dendrites of the representative neurons shown. *Colored arrows* refer to the corresponding blown up region of the dendrite that is *outlined* with the *dotted line* in the same color to the *right*. *B*, FISH using a sense probe (negative control) to verify the specificity of the antisense probe used in *A*. For visualization purposes, the images showing the mRNA puncta were dilated once. *C*, CaMKII α mRNA punctum number was measured in the cell body of DMSO- and rapamycin-treated neurons and normalized by area. DMSO, n=25 neuronal cell bodies, 2000 puncta; Rapa, n=21 neuronal cell bodies, 1544 puncta. *D*, CaMKII α mRNA punctum number was measured in the primary (1°) branch of DMSO- and rapamycin-treated neurons. Note that punctum number is reduced with rapamycin treatment. ***, p<0.01 by unpaired Student's *t* test. DMSO, n=45 primary branches and 212 puncta; Rapa, n=30 primary branches and 68 puncta. *E*, CaMKII α mRNA punctum number was measured in the secondary (2°) branch of DMSO- and rapamycin-treated neurons. Note that punctum number is reduced with rapamycin treatment. ****, p<0.001 by unpaired Student's *t* test. DMSO, n=92 secondary branches and 185 puncta; Rapa, n=60 secondary branches and 36 puncta. *F*, branch variability was determined by counting the number of CaMKII α mRNA puncta in each daughter branch. Quantification of the difference in punctum number between the two branches is shown. ****, p<0.005 by unpaired Student's *t* test. DMSO, n=45 paired daughter branches; Rapa, n=30 paired daughter branches. *G*, CaMKII α mRNA punctum signal intensity was measured in DMSO- and rapamycin-treated neurons from both the primary (10 μ m before the branch point) and the secondary (10 μ m after the branch point) branches. DMSO, n=17 neurons and 26 dendri

alone (Fig. 7, A and B; control, 1.00 \pm 0.21; HuD shRNA, 0.34 \pm 0.12). As a negative control, we used a sense probe that did not detect any signal (Fig. 7C).

To determine whether HuD impacts the subcellular localization of CaMKII α expression, we immunostained control and HuD shRNA-expressing neurons with an antibody against CaMKII α . Notably, the cell body expression was highly variable with no significant overall change between groups of neurons. In contrast, the expression of CaMKII α showed a downward trend in the primary dendrite and a significant decrease in the secondary branches in HuD shRNA-expressing neurons relative to control neurons transfected with vector alone (Fig. 7, E-G; primary dendrite: control, 1.00 ± 0.1 ; HuD shRNA, 0.68 ± 0.13 ; secondary dendrite: control, 1.00 ± 0.08 ; HuD shRNA, 0.87 ± 0.18). Similar to what we observed with our reporter construct, the branch-specific expression of CaMKII α was dramatically reduced by \sim 56% in HuD KD neurons (Fig.

7*G*). Thus, a decrease in HuD expression results in reduced CaMKII α polarized expression with more protein being distributed between daughter branches.

HuD Targets One Daughter Branch over the Other in a Single Neuron—We next examined the possibility that HuD itself may be selectively targeted to one daughter branch over the other and hence mediate the branch-specific expression of CaMKIIα when mTORC1 is active. Because the antibodies available to detect HuD are not reliable for immunofluorescence, we measured HuD protein with an anti-myc antibody directed against the overexpressed myc-tagged HuD protein in hippocampal neurons. Unlike CaMKIIα, total myc-HuD levels did not change with mTORC1 activity as indicated by the quantification of signal in both the primary and the secondary branches (Fig. 8, A–C). Surprisingly, the BVI of myc-HuD more than doubled upon mTORC1 inhibition (HuD, DMSO, 1.00 \pm 0.16; HuD, Rapa, 2.43 \pm 0.37; Fig. 8D).

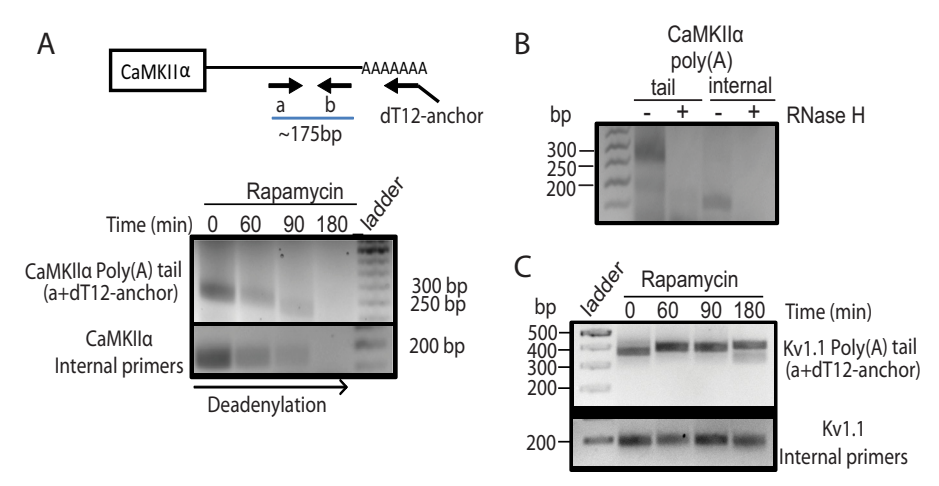


FIGURE 5. mTORC1 inhibition degrades CaMKII α mRNA by deadenylation of its poly(A) tail. A, neurons treated with rapamycin for 0, 60, 90, and 180 min were harvested from cultured neurons, and PCR was performed with specific primers. Top, schematic of CaMKIIα internal primers (a and b) and primers that recognize the poly(A) tail of CaMKII α . Note that CaMKII α poly(A) tail is deadenylated due to mTOR inhibition as indicated by the reduced poly(A) tail length and intensity of the PCR product over time. B. as a control, PCR was performed following RNase H treatment to validate amplification of the PCR product containing the poly(A) tail. C, PCR was performed using Kv1.1-specific primers and primers that recognize the poly(A) tail of Kv1.1. Note that neither the poly(A) tail nor the mRNA levels of Kv1.1 change in rapamycin-treated neurons.

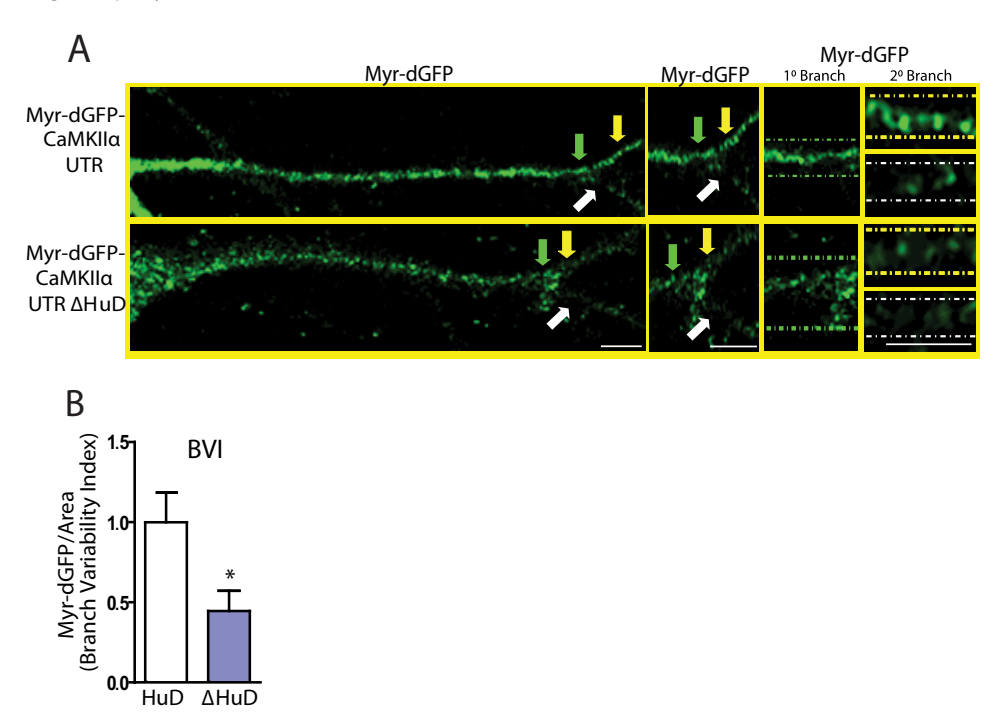


FIGURE 6. Deletion of the HuD binding motifs in the 3'-untranslated region of CaMKII α mRNA prevents its branch-specific expression. A, representative neurons transfected with myr-dGFP-CaMKIIα UTR or myr-dGFP-CaMKIIα UTR ΔHuD and stained for GFP. Colored arrows refer to the corresponding blown up region of the dendrite that is outlined with the dotted line in the same color to the right. B, quantification of neurons transfected with myr-dGFP-CaMKII α UTR or myr-dGFP-CaMKIIa UTR AHuD and stained for GFP. BVI was determined by measuring GFP signal intensity in each daughter branch using the following equation: BVI = |Daughter branch A - Daughter branch B|/Dendritic area. *, p < 0.05 by unpaired Student's t test. myr-dGFP-CaMKII α UTR and myr-dGFP-CaMKII α UTR Δ HuD, n=15 paired daughter branches. Error bars represent S.E. 1°, primary; 2°, secondary. Scale bar represents 10 μ m.

To ensure that HuD overexpression does not increase the diameter of one daughter branch over the other, thus favoring increased protein expression in the larger branch over the smaller branch by diffusion, we measured the diameter of both daughter branches using eGFP in control and HuD-overexpressing neurons. There was no significant difference in the diameter between daughter branches within the same neuron when comparing control and HuD-expressing neurons (Fig. 8E). Collectively, these results suggest that HuD may direct the branch-specific expression of its target mRNAs.

HuD Rescues CaMKIIα Protein Expression and Branch Variability When mTORC1 Is Inhibited—Next, we examined the possibility that overexpression of HuD would increase CaMKIIα protein and hence restore its BVI when mTORC1 is inhibited. We predicted that CaMKIIα BVI would be maintained in HuD-overexpressing neurons in the presence of rapamycin due to the increased targeting of HuD to one daughter branch over the other. Similar to what was observed in Fig. 2, CaMKII α protein levels in the cell body in HuD-overexpressing neurons relative to control neurons remained the same regard-

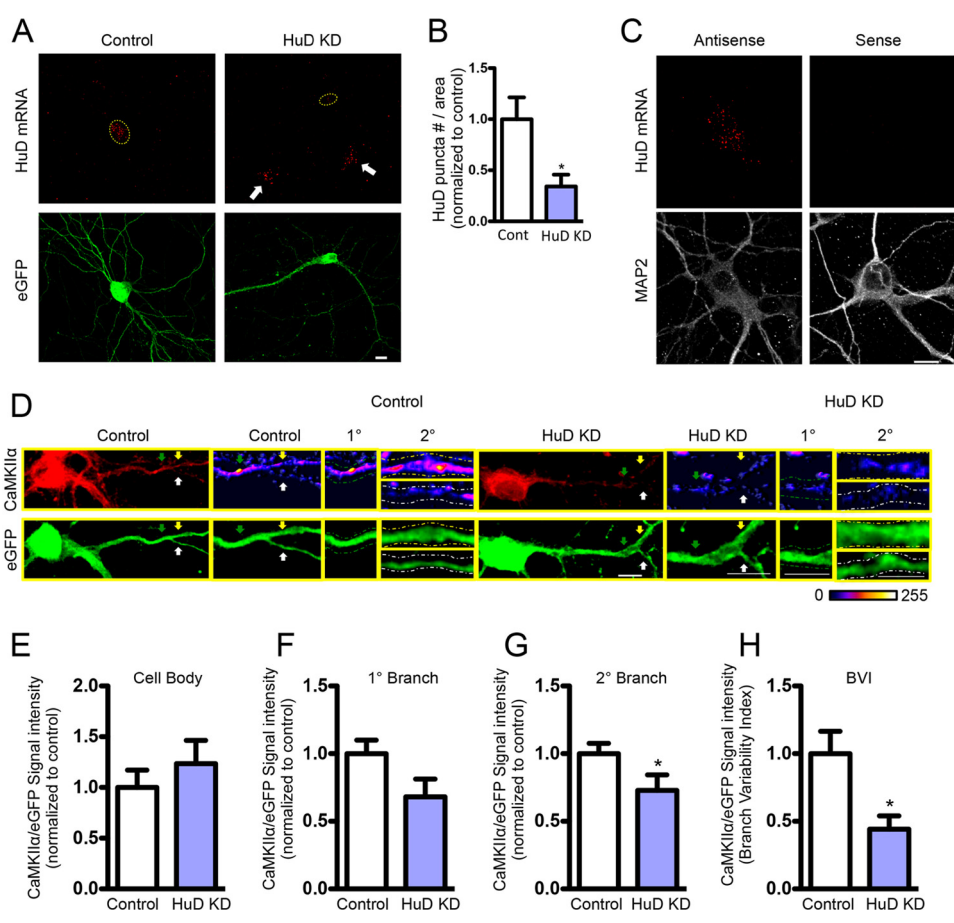


FIGURE 7. Knockdown of endogenous HuD decreases the branch-specific expression of CaMKII α . A, representative images of neurons co-transfected with control vector or shRNA against HuD and eGFP cDNA. 72 h post-transfection, neurons were fixed, and HuD mRNA was detected using an antisense probe set against HuD mRNA. Notice the strong detection of HuD mRNA-containing granule structures in the cell bodies of the control eGFP neuron (left, white dotted outline of cell body) compared with the HuD shRNA (right, white dotted outline of cell body) eGFP neuron. Note that untransfected neurons in the HuD KD panel still express HuD mRNA as indicated by red in situ signal (white arrows). For visualization purposes, the images showing the mRNA puncta were dilated twice. B, quantification of the -fold change of reduced HuD mRNA-containing puncta per area as determined by eGFP signal in the cell body of control (Cont) and shRNA-expressing neurons. Note the \sim 65% reduction in HuD mRNA detection in shRNA-expressing neurons. C, representative neurons showing specificity of the HuD antisense probe set. Note the red in situ punctum signal only with the antisense probe set. D, representative images of CaMKIIa expression in control and HuD shRNA-expressing neurons. Colored arrows refer to the corresponding blown up region of the dendrite that is outlined with the dotted line in the same color to the right. CaMKII α images were also pseudocolored, and three-dimensional rendering was achieved using the Interactive 3D Surface Plot plug-in in ImageJ. E, the signal intensity of CaMKII α in the cell body of control and HuD shRNA-expressing neurons measured as a ratio over eGFP. F, quantification of CaMKII α expression in the primary (1°) branch 10 μ m prior to the branch point. G, quantification of CaMKII α expression in the secondary (2°) branch. Note the non-significant trend in reduced CaMKII α protein levels in the primary dendrite. H, BVI for control and HuD shRNA-expressing neurons. Note the significant reduction in BVI in HuD shRNA neurons compared with control neurons. Significance was determined by Student's t test. *, p < 0.05. Error bars represent S.E. Cell bodies: control, n = 17; HuD KD, n = 10; primary dendrites: control, n = 26; HuD KD, n = 13; branch pairs: control, n = 28; HuD KD, n = 13. Scale bar represents 10 μ m.

less of mTORC1 activity (Fig. 8F). As predicted, in contrast to the cell body, HuD-overexpressing neurons had significantly more CaMKII α protein in the primary dendrite when mTORC1 was inhibited by rapamycin (Fig. 8, A and G). Furthermore, in rapamycin-treated neurons, HuD restored CaMKII α expression back to control levels in the secondary branches (Fig. 8, A and H). Consistent with the increased targeting of HuD when mTORC1 activity was reduced, HuD restored CaMKII α BVI back to control levels (Fig. 8, A and I). These results suggest that HuD increases CaMKII α protein and maintains its BVI when mTORC1 is inhibited.

Branch-specific Expression of CaMKII α Requires the Poly(A) Tail-binding RNA Recognition Motif of HuD—If HuD protects CaMKII α mRNA from deadenylation in a branch-specific manner, then expressing a truncated form of HuD that does not bind to the poly(A) tail of its targets (18, 28, 29) will not rescue

CaMKII α BVI. HuD has three RNA recognition motifs (RRMs), two of which bind specific HuD binding motifs in the mRNA sequence of its targets. The third RRM binds the poly(A) tail of its mRNA targets (28, 29). Because shortening of the CaMKII α poly(A) tail led to mRNA degradation, we examined whether the third RRM and linker region of HuD are required to mediate the HuD-dependent rescue of CaMKIIα BVI when mTORC1 is inhibited. Indeed, overexpression of a HuD construct lacking the third RRM (HuD I+II) alone did not block the reduction of CaMKIIα protein or BVI as had the full-length protein when mTORC1 was inhibited (Fig. 8, A and F-I). Interestingly, in HuD I+II-expressing neurons, CaMKII α levels were high when mTORC1 was active, and the expression of HuD remained polarized (myc HuD, Fig. 8, C and D; CaMKII α , Fig. 8, G and H). Unexpectedly, the ability of HuD to mediate branch-specific expression of CaMKII α was greatly reduced (Fig. 8, A and I, red

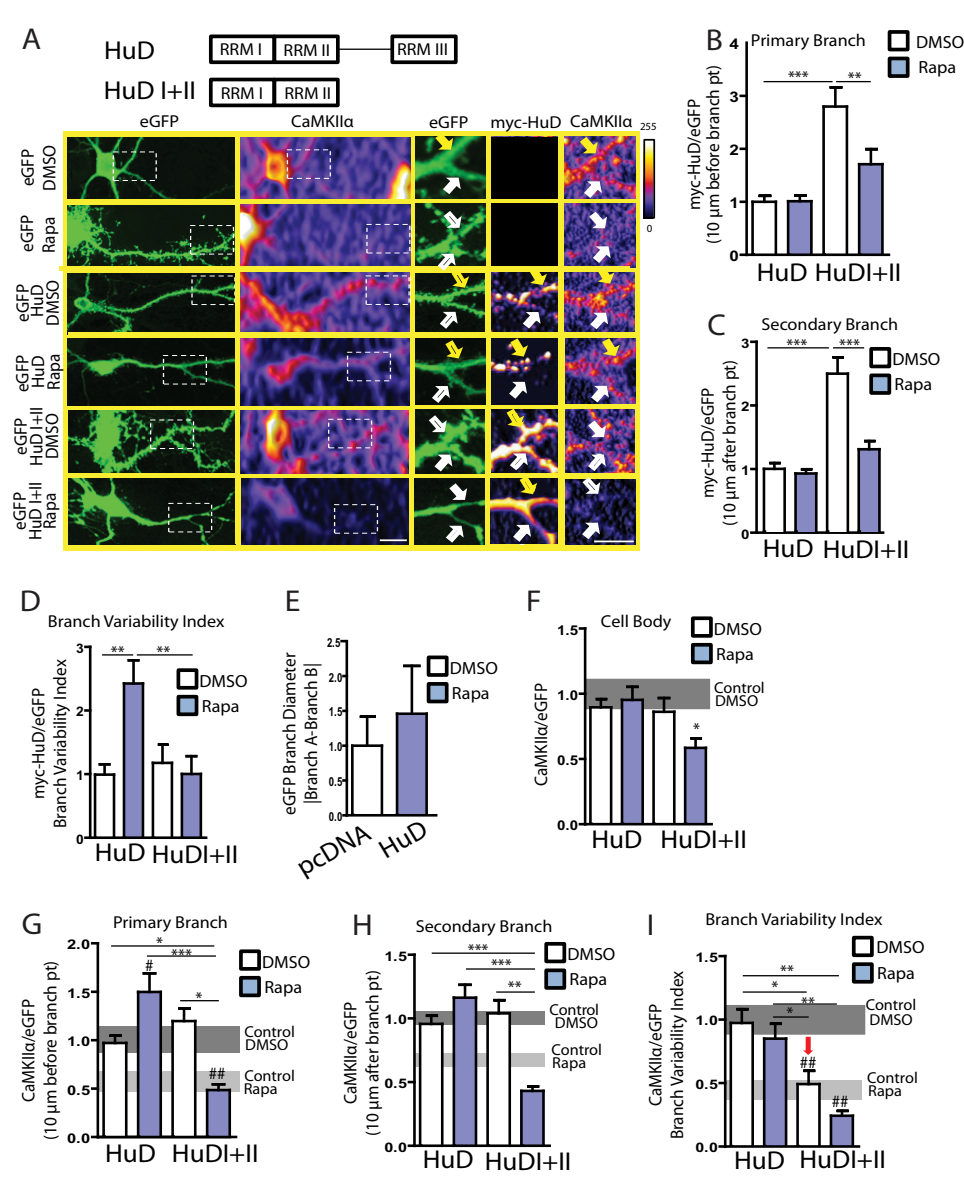


FIGURE 8. Differential branch expression of full-length myc-HuD but not its truncated form missing the domain that binds the poly(A) tail rescues CaMKII a branch variability when mTORC1 is inhibited. Ā, top, schematic showing HuD constructs used. Cultured hippocampal neurons were transfected with pcDNA+eGFP, pcHuD+eGFP, or pcHuD+II+eGFP and treated with either carrier (DMSO) or rapamycin. Representative neurons immunostained for CaMKII α and myc-HuD are shown. Dotted box indicates blown up branch points to the right. Scale bar represents $10 \mu m$. CaMKII α and myc-HuD images were also pseudocolored, and three-dimensional rendering was achieved using the Interactive 3D Surface Plot plug-in in ImageJ. A yellow arrows indicates a daughter branch with more HuD and CaMKIIa protein relative to the other daughter branch (white arrow). Scale bar, 10 µm. B, primary (10 µm before branch point) dendritic myc-HuD protein was measured as a ratio over eGFP. HuD DMSO, n = 11 primary dendrites; HuD Rapa, 13 primary dendrites; HuD I+II DMSO, n = 15 primary branches; HuD I+II Rapa, n = 15 primary branches; HuD I+II Rap 10 primary branches. **, p < 0.01; ***, p < 0.005 by one-way ANOVA Newman-Keuls post-test. C, myc-HuD protein in secondary daughter branches (10 μ m after the branch point) was measured as a ratio over eGFP. $\frac{1}{2}$ HuD DMSO, n=22 secondary branches; $\frac{1}{2}$ branch point) was measured as a ratio over eGFP. $\frac{1}{2}$ HuD DMSO, n=30 secondary branches; $\frac{1}{2}$ branches; $\frac{$ branches; $\text{HuD}\,\text{I}+\text{II}\,\text{Rapa}, n=20$ secondary branches.***, p<0.005 by one-way ANOVA Newman-Keuls post-test. D, myc-HuD/eGFP protein was subtracted between daughter branches and normalized to $\text{myc-HuD}\,\text{DMSO}$ and graphed as BVI. Note the increased BVI for myc-HuD between daughter branches in rapamycin-treated neurons. **, p < 0.01 by one-way ANOVA Newman-Keuls post-test. HuD DMSO, n = 11 paired daughter branches; HuD Rapa, 11 paired daughter branches; HuD I+II DMSO, n = 15 paired daughter branches; HuD I+II Rapa, n = 10 paired daughter branches. E, the difference in diameter between daughter branches of neurons transfected with eGFP+pcDNA or eGFP+myc-HuD was measured using eGFP. Note there is no significant difference in branch diameter between pcDNA and myc-HuD neurons. pcDNA, n=10 secondary branches; HuD, n=20 secondary branches. F, CaMKII α protein was measured in the cell body of HuD- or HuD I+II-transfected neurons that were then DMSO- or rapamycin-treated. HuD DMSO, n=27; HuD Rapa, n=24; HuD I+II DMSO, n=16; HuD I+II Rapa, n=15.*, p<0.05by one-way ANOVA Newman-Keuls post-test. G, primary dendritic CaMKII α protein (10 μ m before branch point) was measured as a ratio over eGFP. Note that HuD rescues reduced CaMKII α levels in rapamycin-treated neurons. #, p < 0.05; ##, p < 0.01 significantly different from pcDNA DMSO by one-sample t test. *, p < 0.05; ***, p < 0.005 by one-way ANOVA Newman-Keuls post-test. HuD DMSO, n = 26 primary dendrites; HuD Rapa, 25 primary dendrites; HuD I+II DMSO, n = 19 primary dendrites; HuDI+II Rapa, n=14 primary dendrites. The *dark gray bar* represents the mean \pm S.E. of pcDNA DMSO neurons as determined in Fig. 2. The *light gray bar* represents the mean \pm S.E. of pcDNA Rapa neurons as determined in Fig. 2. H, CaMKII α protein in secondary daughter branches (secondary branch; 10 μ m after the branch point) was measured as a ratio over eGFP.**, p < 0.01; ***, p < 0.005 by one-way ANOVA Newman-Keuls post-test. HuD DMSO, n = 78 secondary branches; HuD I+II DMSO, n = 36 secondary branches; HuD I+II Rapa, n = 30 secondary branches. l, the absolute value of the difference between $CaMKII\alpha/eGFP\ protein\ was\ subtracted\ between\ daughter\ branches\ and\ normalized\ to\ pcDNA\ DMSO\ BVI\ and\ graphed\ as\ BVI.\ Note\ that\ HuD\ rescues\ reduced\ CaMKII\alpha/eGFP\ protein\ was\ subtracted\ between\ daughter\ branches\ and\ normalized\ to\ pcDNA\ DMSO\ BVI\ and\ graphed\ as\ BVI.\ Note\ that\ HuD\ rescues\ reduced\ CaMKII\alpha/eGFP\ protein\ was\ subtracted\ between\ daughter\ branches\ and\ normalized\ to\ pcDNA\ DMSO\ BVI\ and\ graphed\ as\ BVI.\ Note\ that\ HuD\ rescues\ reduced\ CaMKII\alpha/eGFP\ protein\ was\ subtracted\ between\ daughter\ branches\ and\ normalized\ to\ pcDNA\ DMSO\ BVI\ and\ graphed\ as\ BVI.\ Note\ that\ HuD\ rescues\ reduced\ CaMKII\alpha/eGFP\ protein\ was\ subtracted\ between\ daughter\ branches\ daughte$ BVI when mTOR is inhibited. In addition, removing the linker region and third RRM significantly reduces the branch-specific expression of CaMKII α when mTORC1 is active (red arrow). ##, p < 0.01, significantly different from DMSO control, as determined by a single t-test. *, p < 0.05; **, < 0.01 by one-way ANOVA Newman-Keuls post-test. HuD DMSO, n = 36 paired daughter branches; HuD Rapa, n = 44 paired daughter branches; HuD I+II DMSO, n = 18 paired daughter branches; HuD I+II Rapa, n = 15 paired daughter branches. Error bars represent S.E.

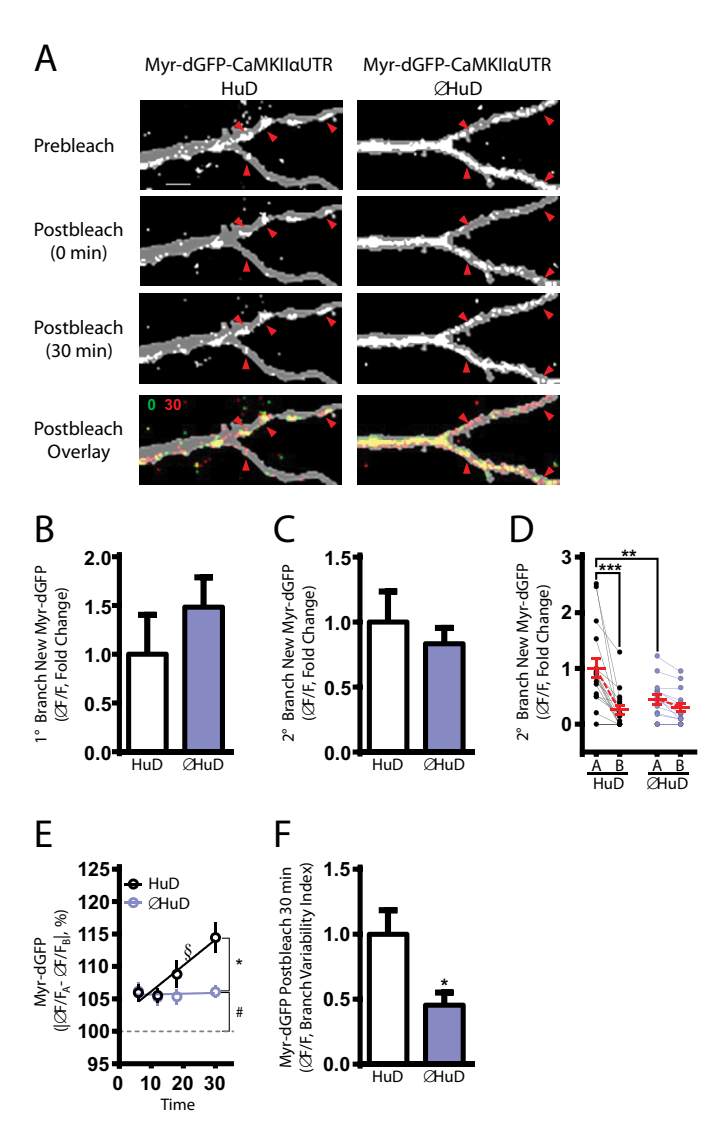


FIGURE 9. Fluorescence recovery after photobleaching of myristoylated dGFP-CaMKIIlpha UTR demonstrates that HuD binding sites facilitate branch-specific local synthesis. A, representative images of dendrites expressing myr-dGFP fused to CaMKII α UTR in which HuD binding sites are maintained (HuD; left) or deleted (ΔHuD; right). dGFP fluorescence of the same dendrites before (top), immediately after (0 min), and 30 min after photobleaching. The bottom panel is an overlay of dGFP at 0 (green) and 30 min (red). Yellow indicates unbleached dGFP. After 30 min of recovery, myr-dGFP-CaMKII α UTR HuD displays polarized translation of dGFP, whereas myr-dGFP-CaMKII α -UTR Δ HuD shows approximately equal dGFP translation. Red arrowheads indicate GFP signals that disappear or are reduced immediately after bleaching (time 0) and reappear 30 min after recovery. dGFP signals are overlaid on their respective dendrites (gray). Scale bar, 10 μ m. B and C, deletion of HuD binding sites does not affect the total expression of new myr-dGFP in primary (B) (HuD = 1.00 ± 0.40 ; $\Delta \text{HuD} = 1.48 \pm 0.31$; p = 0.35) and secondary (C) (HuD = 1.00 ± 0.23 ; Δ HuD = 0.83 ± 0.12 ; p = 0.55) dendrites 30 min after bleaching. D, deletion of HuD binding sites reduces polarized translation between daughter dendrites that emerge from a single primary dendrite. Dendrite A is assigned to a daughter dendrite that expresses more dGFP, and dendrite B is assigned to a daughter dendrite that expresses less dGFP. Data points of designated A and B daughter dendrites in a single neuron are connected by dotted lines (HuD A = 1.00 \pm 0.17; HuD B = 0.26 \pm 0.08; Δ HuD A = 0.44 ± 0.09 ; $\Delta HuD B = 0.30 \pm 0.08$). At 30 min after recovery, HuD daughter dendrites display more polarized expression of new dGFP than Δ HuD daughter dendrites (+HuD A-B, p < 0.0001; Δ HuD A-B, p = 0.8389; one-way ANOVA, Tukey's multiple comparison test). Dendrites designated A (highly expressing daughter dendrites) with HuD binding sites contain more dGFP than ΔHuDexpressing cells (HuD A = 1.00 \pm 0.17; Δ HuD A = 0.44 \pm 0.09; p < 0.006; one-way ANOVA, Tukey's multiple comparison test). E, new myr-dGFP protein synthesis is observed after 6 min of recovery in both reporter constructs ($\dot{H}uD = 105.9 \pm 1.3\%$; $\Delta HuD = 106.2 \pm 1.3\%$; $\dot{\#}$, p < 0.006 by Student's t test

arrow). These findings suggest that binding of the poly(A) tail to the third RRM of HuD underlies the differential expression of CaMKII α between daughter branches.

Branch-specific Local Translation of a CaMKII\alpha Reporter Requires HuD mRNA Binding Sites—Because HuD mediated the polarized expression of CaMKII α mRNA, we hypothesized that $CaMKII\alpha$ mRNA local translation is also branch-specific. To test our hypothesis, we performed fluorescence recovery after photobleaching of our reporters, myristoylated dGFP fused to the 3'-UTR of CaMKIIα in which HuD binding sites were maintained (myr-dGFP-CaMKIIα UTR HuD) or removed (myr-dGFP-CaMKII α UTR Δ HuD) (Fig. 6) (23, 24, 31). We then measured the translation-dependent recovery from photobleaching of each reporter construct. An increase in fluorescence during recovery represents newly synthesized dGFP protein (Fig. 9A, red arrows) (31). Because dGFP contains a myristoylation site, which tethers the protein to the membrane and thus limits protein movement, increased dGFP fluorescence is due to local protein synthesis and not protein diffusion (23, 24, 31). Removal of HuD binding sites did not alter the total expression of new myr-dGFP in the primary and secondary dendrites at 30 min of recovery (primary: $HuD = 1.00 \pm 0.40$, $\Delta HuD = 1.48 \pm 0.31$; secondary: $+HuD = 1.00 \pm 0.23$, Δ HuD = 0.83 \pm 0.12; Fig. 9, *B* and *C*). However, dendrite A, a daughter dendrite conventionally assigned as expressing more dGFP, with the HuD binding sites contained more dGFP than dendrite A without the HuD binding sites (HuD A = $1.00 \pm$ 0.17; Δ HuD A = 0.44 \pm 0.09; Fig. 9*D*). Dendrite B, a daughter dendrite designated as expressing less myr-dGFP, exhibited similar levels of new myr-dGFP protein, regardless of the presence of HuD binding sites (+HuD B = 0.26 ± 0.08 ; Δ HuD B = 0.30 ± 0.08 ; Fig. 9C). Additionally, the levels of new myr-dGFP between HuD daughter dendrites A and B are significantly polarized compared with Δ HuD daughter dendrites (HuD A-B, p < 0.0001; Δ HuD A-B, p = 0.8389; one-way ANOVA, Tukey's multiple comparison test). These findings suggest that between daughter branches the presence of HuD binding sites generally supports the polarized, dendritic translation of myr-dGFP-CaMKII α mRNA.

For both reporters, we detected comparable syntheses of new myr-dGFP proteins at 6 min after photobleaching as we saw a significant increase in fluorescence compared with baseline (F_0), the fluorescence intensity immediately after photobleaching (HuD = $105.9 \pm 1.3\%$; Δ HuD = $106.2 \pm 1.3\%$; Fig. 9*E*). The difference in new myr-dGFP synthesis between +HuD daughter dendrites remarkably increased throughout the recovery period, demonstrating that one daughter dendrite has a higher

compared with baseline (dashed line)) Baseline is fluorescence intensity immediately after photobleaching (time = 0 min; F_0). Removing HuD binding sites abrogates the polarized new translation of myr-dGFP between daughter dendrites (HuD slope = 0.40 \pm 0.11; Δ HuD slope = 0.01 \pm 0.06). Slopes were determined by linear regression analysis (§, p < 0.003). 30 min after photobleaching, HuD daughter dendrites exhibit greater polarity in myr-dGFP expression compared with Δ HuD daughter dendrites (HuD = 114.5 \pm 2.4%; Δ HuD = 106.1 \pm 1.0%; *, p < 0.003). F, deletion of HuD binding sites reduces dendritic BVI of new myr-dGFP protein after 30 min of recovery (HuD = 1.00 \pm 1.5; Δ HuD = 0.48 \pm 0.1; p < 0.007). n = 11 neurons for myr-dGFP-CaMKIl α UTR HuD; n = 10 for myr-dGFP-CaMKIl α UTR Δ HuD. Student's t test was used for statistical analyses for B, C, and E. Error bars represent S.E. 1°, primary; 2°, secondary. *, p < 0.05; **, p < 0.01; ***, p < 0.001.



translation rate than the other (HuD slope = 0.40 ± 0.11 ; Fig. 9*E*). In Δ HuD, however, the difference in new myr-dGFP translation between daughter branches was abrogated, indicating that daughter branches exhibited equal translation (Δ HuD slope = 0.01 ± 0.06 ; Fig. 9*E*). Compared with Δ HuD-expressing neurons, HuD cells exhibited more polarity in fluorescence or new myr-dGFP proteins in one daughter branch over the other at 30 min after recovery (+HuD = $114.5 \pm 2.4\%$; Δ HuD = $106.1 \pm 1.0\%$; Fig. 9*E*). Deletion of HuD binding sites likewise reduced the BVI of newly translated myr-dGFP (+HuD = 1.00 ± 1.5 ; Δ HuD = 0.48 ± 0.1 ; Fig. 9*F*). These results altogether demonstrate that HuD binding sites mediate the polarized translation of myr-dGFP-CaMKII α UTR.

Discussion

The temporal and spatial regulation of protein expression is critical for a neuron to modify its synaptic input in an experience-dependent manner (32, 33). "Synaptic tag and capture" in which proteins localized in response to strong stimuli at one set of synapses are available to other nearby synapses to facilitate plasticity at both sets of synapses is thought to underlie long-term plasticity (14). Synapses that are "bound" together and distributed on a single dendritic branch increase the probability that excitatory postsynaptic potential amplification will occur (34–37). Molecular mechanisms that mediate branch-specific expression of proteins that facilitate plasticity are unknown.

We used a simplified model in which dendritic mTORC1 is active and can be inhibited with rapamycin to ask whether phosphorylated mTORC1 can serve as a tag. We determined that mTORC1 is active in both daughter branches by NMDAR activity (Fig. 1), a specified requirement to serve as a tag during late stage plasticity (15). Interestingly, NMDAR/mTOR activity only mediated the selective expression of the plasticity-related protein CaMKII α in one branch. We discovered that HuD, the RNA-binding protein that has been characterized previously to stabilize CaMKII α mRNA and promote its translation (38), mediates its branch-specific expression by targeting its mRNA to one daughter branch over the other. Deletion of the HuD binding sites in the 3'-UTR of CaMKII α mRNA abrogated its branch-specific local expression (Figs. 6 and 9).

We have shown that degradation of CaMKII α mRNA occurs through deadenylation when mTORC1 activity is reduced and may explain the rapamycin-dependent reduction in CaMKII α branch variability. Remarkably, HuD overexpression protected and rescued the rapamycin-reduction in CaMKIIα protein, confirming that HuD is limited when mTORC1 activity is reduced (5). As predicted, overexpression of HuD I+II, notably missing the third RRM that binds to the poly(A) tail, failed to rescue CaMKIIα protein and BVI reduction when mTORC1 was inhibited. Although our evidence is strong for changes in mRNA abundance reflecting changes in protein expression, we cannot discount the fact that there may be corresponding changes in $CaMKII\alpha$ protein stability. It should be noted that mTORC1 inhibition also promotes autophagy (39), suggesting that mTORC1 is an important signaling pathway in protein homeostasis.

One of the most surprising results herein is that the absence of HuD binding to the poly(A) tail resulted in the equal distribution of CaMKII α protein in both daughter branches, suggesting that poly(A) binding is required to mediate CaMKII α branch-specific expression. These results lead to the intriguing possibility that the length of the poly(A) tail of plasticity-related mRNAs may serve as the bait for HuD capture and branch-selective expression.

Redondo and Morris (15) have suggested that there may be multiple tags that can facilitate synaptic capture of plasticity-related proteins. Consistent with this idea, previous reports have suggested that CaMKII α itself serves as a tag. Notably, inhibiting the phosphorylation of CaMKII α prevents late phase LTP, a requirement to serve as a tag (40). Although we did not detect CaMKII α in both branches, blocking CaMKII α activity in activated synapses where it is localized may be sufficient to block long term changes in plasticity. Through the discovery of HuD as the RNA-binding protein that mediates CaMKII α expression herein, future experiments may help elucidate the tag/plasticity-related protein interactions in more complex systems.

The question of how specific mRNAs target activated synapses is perplexing. It has been suggested that neuronal ribonucleoproteins patrol a group of synapses (41). Consistent with this idea, bidirectional movement of mRNAs in dendrites has been observed (41–45). Global mRNA "exploration" may be required for the local protein synthesis at stimulated synapses during early events that set the stage for long term plasticity (46, 47). Interestingly, HuD protein levels increase with neuronal/mTORC1 activity (5, 48), and the protein is targeted in a branch-specific manner. Collectively, these data suggest that HuD is a good candidate to target the mRNAs coding for proteins required to strengthen neighboring synapses to facilitate late stage plasticity.

In summary, our previous study demonstrating that HuD can switch target mRNAs from CaMKII α when mTORC1 is active to Kv1.1 when mTORC1 is inhibited combined with these findings suggests that the branch-specific expression of HuD may be what "captures" mRNAs to specifically shuttle and stabilize them in one daughter branch based on their affinity and abundance. How HuD protein targets one daughter branch over the other in a single neuron is yet to be determined. However, what is clear is that the mRNA that it captures, be it CaMKII α mRNA when mTORC1 is active or Kv1.1 mRNA when mTORC1 activity is reduced, will depend on the level of mTORC1 activity, serving as the tag and dictating the strength of the synapse (5, 41).

Acknowledgment—We thank Dr. Erin Schuman for kindly providing the myr-dGFP-CaMKII α UTR cDNA.

References

- Blundell, J., Kouser, M., and Powell, C. M. (2008) Systemic inhibition of mammalian target of rapamycin inhibits fear memory reconsolidation. Neurobiol. Learn. Mem. 90, 28 – 35
- Graber, T. E., Hébert-Seropian, S., Khoutorsky, A., David, A., Yewdell, J. W., Lacaille, J. C., and Sossin, W. S. (2013) Reactivation of stalled polyribosomes in synaptic plasticity. *Proc. Natl. Acad. Sci. U.S.A.* 110,



- 16205-16210
- Hay, N., and Sonenberg, N. (2004) Upstream and downstream of mTOR. Genes Dev. 18, 1926–1945
- Gong, R., Park, C. S., Abbassi, N. R., and Tang, S. J. (2006) Roles of glutamate receptors and the mammalian target of rapamycin (mTOR) signaling pathway in activity-dependent dendritic protein synthesis in hippocampal neurons. *J. Biol. Chem.* 281, 18802–18815
- Sosanya, N. M., Huang, P. P., Cacheaux, L. P., Chen, C. J., Nguyen, K., Perrone-Bizzozero, N. I., and Raab-Graham, K. F. (2013) Degradation of high affinity HuD targets releases Kv1.1 mRNA from miR-129 repression by mTORC1. J. Cell Biol. 202, 53–69
- Mayford, M., Bach, M. E., Huang, Y. Y., Wang, L., Hawkins, R. D., and Kandel, E. R. (1996) Control of memory formation through regulated expression of a CaMKII transgene. *Science* 274, 1678–1683
- Miller, S., Yasuda, M., Coats, J. K., Jones, Y., Martone, M. E., and Mayford, M. (2002) Disruption of dendritic translation of CaMKIIα impairs stabilization of synaptic plasticity and memory consolidation. *Neuron* 36, 507–519
- Govindarajan, A., Israely, I., Huang, S. Y., and Tonegawa, S. (2011) The dendritic branch is the preferred integrative unit for protein synthesis-dependent LTP. Neuron 69, 132–146
- Bolognani, F., Merhege, M. A., Twiss, J., and Perrone-Bizzozero, N. I. (2004) Dendritic localization of the RNA-binding protein HuD in hippocampal neurons: association with polysomes and upregulation during contextual learning. *Neurosci. Lett.* 371, 152–157
- Bolognani, F., Qiu, S., Tanner, D. C., Paik, J., Perrone-Bizzozero, N. I., and Weeber, E. J. (2007) Associative and spatial learning and memory deficits in transgenic mice overexpressing the RNA-binding protein HuD. *Neuro-biol. Learn. Mem.* 87, 635–643
- Pascale, A., Gusev, P. A., Amadio, M., Dottorini, T., Govoni, S., Alkon, D. L., and Quattrone, A. (2004) Increase of the RNA-binding protein HuD and posttranscriptional up-regulation of the GAP-43 gene during spatial memory. *Proc. Natl. Acad. Sci. U.S.A.* 101, 1217–1222
- Mahan, A. L., Mou, L., Shah, N., Hu, J. H., Worley, P. F., and Ressler, K. J. (2012) Epigenetic modulation of Homer1a transcription regulation in amygdala and hippocampus with pavlovian fear conditioning. *J. Neurosci.* 32, 4651–4659
- Routtenberg, A., Cantallops, I., Zaffuto, S., Serrano, P., and Namgung, U. (2000) Enhanced learning after genetic overexpression of a brain growth protein. *Proc. Natl. Acad. Sci. U.S.A.* 97, 7657–7662
- Frey, U., and Morris, R. G. (1997) Synaptic tagging and long-term potentiation. *Nature* 385, 533–536
- 15. Redondo, R. L., and Morris, R. G. (2011) Making memories last: the synaptic tagging and capture hypothesis. *Nat. Rev. Neurosci.* **12**, 17–30
- Cammalleri, M., Lütjens, R., Berton, F., King, A. R., Simpson, C., Francesconi, W., and Sanna, P. P. (2003) Time-restricted role for dendritic activation of the mTOR-p70S6K pathway in the induction of late-phase long-term potentiation in the CA1. *Proc. Natl. Acad. Sci. U.S.A.* 100, 14368–14373
- Tang, S. J., Reis, G., Kang, H., Gingras, A. C., Sonenberg, N., and Schuman, E. M. (2002) A rapamycin-sensitive signaling pathway contributes to longterm synaptic plasticity in the hippocampus. *Proc. Natl. Acad. Sci. U.S.A.* 99, 467–472
- Anderson, K. D., Morin, M. A., Beckel-Mitchener, A., Mobarak, C. D., Neve, R. L., Furneaux, H. M., Burry, R., and Perrone-Bizzozero, N. I. (2000) Overexpression of HuD, but not of its truncated form HuD I+II, promotes GAP-43 gene expression and neurite outgrowth in PC12 cells in the absence of nerve growth factor. *J. Neurochem.* 75, 1103–1114
- Cajigas, I. J., Tushev, G., Will, T. J., tom Dieck, S., Fuerst, N., and Schuman, E. M. (2012) The local transcriptome in the synaptic neuropil revealed by deep sequencing and high-resolution imaging. *Neuron* 74, 453–466
- Udagawa, T., Swanger, S. A., Takeuchi, K., Kim, J. H., Nalavadi, V., Shin, J., Lorenz, L. J., Zukin, R. S., Bassell, G. J., and Richter, J. D. (2012) Bidirectional control of mRNA translation and synaptic plasticity by the cytoplasmic polyadenylation complex. *Mol. Cell* 47, 253–266
- 21. Wu, L., Wells, D., Tay, J., Mendis, D., Abbott, M. A., Barnitt, A., Quinlan, E., Heynen, A., Fallon, J. R., and Richter, J. D. (1998) CPEB-mediated

- cytoplasmic polyadenylation and the regulation of experience-dependent translation of α -CaMKII mRNA at synapses. *Neuron* **21,** 1129 –1139
- Ratti, A., Fallini, C., Colombrita, C., Pascale, A., Laforenza, U., Quattrone, A., and Silani, V. (2008) Post-transcriptional regulation of neuro-oncological ventral antigen 1 by the neuronal RNA-binding proteins ELAV. J. Biol. Chem. 283, 7531–7541
- Aakalu, G., Smith, W. B., Nguyen, N., Jiang, C., and Schuman, E. M. (2001)
 Dynamic visualization of local protein synthesis in hippocampal neurons. Neuron 30, 489 –502
- Sutton, M. A., Wall, N. R., Aakalu, G. N., and Schuman, E. M. (2004)
 Regulation of dendritic protein synthesis by miniature synaptic events. Science 304, 1979 –1983
- Raab-Graham, K. F., Haddick, P. C., Jan, Y. N., and Jan, L. Y. (2006) Activity- and mTOR-dependent suppression of Kv1.1 channel mRNA translation in dendrites. Science 314, 144–148
- Sosanya, N. M., Brager, D. H., Wolfe, S., Niere, F., and Raab-Graham, K. F.
 (2015) Rapamycin reveals an mTOR-independent repression of Kv1.1 expression during epileptogenesis. *Neurobiol. Dis.* 73, 96–105
- Albig, A. R., and Decker, C. J. (2001) The target of rapamycin signaling pathway regulates mRNA turnover in the yeast *Saccharomyces cerevisiae*. *Mol. Biol. Cell* 12, 3428 – 3438
- Beckel-Mitchener, A. C., Miera, A., Keller, R., and Perrone-Bizzozero, N. I. (2002) Poly(A) tail length-dependent stabilization of GAP-43 mRNA by the RNA-binding protein HuD. J. Biol. Chem. 277, 27996–28002
- 29. Ma, W. J., Chung, S., and Furneaux, H. (1997) The Elav-like proteins bind to AU-rich elements and to the poly(A) tail of mRNA. *Nucleic Acids Res.* **25**, 3564–3569
- Bolognani, F., Contente-Cuomo, T., and Perrone-Bizzozero, N. I. (2010)
 Novel recognition motifs and biological functions of the RNA-binding protein HuD revealed by genome-wide identification of its targets. *Nucleic Acids Res.* 38, 117–130
- Merianda, T. T., Gomes, C., Yoo, S., Vuppalanchi, D., and Twiss, J. L. (2013) Axonal localization of neuritin/CPG15 mRNA in neuronal populations through distinct 5' and 3' UTR elements. *J. Neurosci.* 33, 13735–13742
- Govindarajan, A., Kelleher, R. J., and Tonegawa, S. (2006) A clustered plasticity model of long-term memory engrams. *Nat. Rev. Neurosci.* 7, 575–583
- 33. Kandel, E. R. (2001) The molecular biology of memory storage: a dialogue between genes and synapses. *Science* **294**, 1030 –1038
- Harnett, M. T., Makara, J. K., Spruston, N., Kath, W. L., and Magee, J. C. (2012) Synaptic amplification by dendritic spines enhances input cooperativity. *Nature* 491, 599 – 602
- Losonczy, A., Makara, J. K., and Magee, J. C. (2008) Compartmentalized dendritic plasticity and input feature storage in neurons. *Nature* 452, 436 – 441
- Makara, J. K., Losonczy, A., Wen, Q., and Magee, J. C. (2009) Experience-dependent compartmentalized dendritic plasticity in rat hippocampal CA1 pyramidal neurons. *Nat. Neurosci.* 12, 1485–1487
- Makino, H., and Malinow, R. (2011) Compartmentalized versus global synaptic plasticity on dendrites controlled by experience. *Neuron* 72, 1001–1011
- Deschênes-Furry, J., Perrone-Bizzozero, N., and Jasmin, B. J. (2006) The RNA-binding protein HuD: a regulator of neuronal differentiation, maintenance and plasticity. *BioEssays* 28, 822–833
- Wullschleger, S., Loewith, R., and Hall, M. N. (2006) TOR signaling in growth and metabolism. Cell 124, 471–484
- Redondo, R. L., Okuno, H., Spooner, P. A., Frenguelli, B. G., Bito, H., and Morris, R. G. (2010) Synaptic tagging and capture: differential role of distinct calcium/calmodulin kinases in protein synthesis-dependent longterm potentiation. *J. Neurosci.* 30, 4981–4989
- 41. Doyle, M., and Kiebler, M. A. (2011) Mechanisms of dendritic mRNA transport and its role in synaptic tagging. *EMBO J.* **30**, 3540–3552
- Dictenberg, J. B., Swanger, S. A., Antar, L. N., Singer, R. H., and Bassell, G. J. (2008) A direct role for FMRP in activity-dependent dendritic mRNA transport links filopodial-spine morphogenesis to fragile X syndrome. Dev. Cell 14, 926–939
- 43. Dynes, J. L., and Steward, O. (2007) Dynamics of bidirectional transport of



- Arc mRNA in neuronal dendrites. J. Comp. Neurol. 500, 433-447
- Knowles, R. B., Sabry, J. H., Martone, M. E., Deerinck, T. J., Ellisman, M. H., Bassell, G. J., and Kosik, K. S. (1996) Translocation of RNA granules in living neurons. *J. Neurosci.* 16, 7812–7820
- 45. Köhrmann, M., Luo, M., Kaether, C., DesGroseillers, L., Dotti, C. G., and Kiebler, M. A. (1999) Microtubule-dependent recruitment of Staufengreen fluorescent protein into large RNA-containing granules and subsequent dendritic transport in living hippocampal neurons. *Mol. Biol. Cell* 10, 2945–2953
- Farris, S., Lewandowski, G., Cox, C. D., and Steward, O. (2014) Selective localization of arc mRNA in dendrites involves activity- and translationdependent mRNA degradation. *J. Neurosci.* 34, 4481–4493
- 47. Kim, S., and Martin, K. C. (2015) Neuron-wide RNA transport combines with netrin-mediated local translation to spatially regulate the synaptic proteome. *Elife* 4
- Tiruchinapalli, D. M., Ehlers, M. D., and Keene, J. D. (2008) Activity-dependent expression of RNA binding protein HuD and its association with mRNAs in neurons. RNA Biol. 5, 157–168



Mammalian Target of Rapamycin (mTOR) Tagging Promotes Dendritic Branch Variability through the Capture of Ca $^{2+}$ /Calmodulin-dependent Protein Kinase II α (CaMKII α) mRNAs by the RNA-binding Protein HuD

Natasha M. Sosanya, Luisa P. Cacheaux, Emily R. Workman, Farr Niere, Nora I. Perrone-Bizzozero and Kimberly F. Raab-Graham

J. Biol. Chem. 2015, 290:16357-16371. doi: 10.1074/jbc.M114.599399 originally published online May 5, 2015

Access the most updated version of this article at doi: 10.1074/jbc.M114.599399

Alerts:

- · When this article is cited
- · When a correction for this article is posted

Click here to choose from all of JBC's e-mail alerts

This article cites 47 references, 24 of which can be accessed free at http://www.jbc.org/content/290/26/16357.full.html#ref-list-1